Frontiers of Physics
https://doi.org/10.1007/s11467-021-1107-4
Front. Phys.
17(2), 23202 (2022)

TOPICAL REVIEW

Thermal conductivity of micro/nano-porous polymers: Prediction models and applications

Haiyan Yu[1], Haochun Zhang[1,†], Jinchuan Zhao[2,3], Jing Liu[2], Xinlin Xia[1], Xiaohu Wu[4]

[1] *School of Energy Science and Engineering, Harbin Institute of Technology, Harbin 150001, China*
[2] *Microcellular Plastics Manufacturing Laboratory (MPML), Department of Mechanical & Industrial Engineering, University of Toronto, 5 King's College Road, Toronto, M5S 3G8, Ontario, Canada*
[3] *Cellular Polymer Science & Technology Laboratory, School of Materials Science & Engineering, Shandong University, Jinan 250061, China*
[4] *Shandong Institute of Advanced Technology, Jinan 250100, China*
Corresponding author. E-mail: [†] *hczhang@hit.edu.cn*
Received October 20, 2020; accepted July 16, 2021

Micro/nano-porous polymeric material is considered a unique industrial material due to its extremely low thermal conductivity, low density, and high surface area. Therefore, it is necessary to establish an accurate thermal conductivity prediction model suiting their applicable conditions and provide a theoretical basis for expanding their applications. In this work, the development of the calculation model of equivalent thermal conductivity of micro/nano-porous polymeric materials in recent years is summarized. Firstly, it reviews the process of establishing the overall equivalent thermal conductivity calculation model for micro/nanoporous polymers. Then, the predicted calculation models of thermal conductivity are introduced separately according to the conductive and radiative thermal conductivity models. In addition, the thermal conduction part is divided into the gaseous thermal conductivity model, solid thermal conductivity model and gas–solid coupling model. Finally, it is concluded that, compared with other porous materials, there are few studies on heat transfer of micro/nanoporous polymers, especially on the particular heat transfer mechanisms such as scale effects at the micro/nanoscale. In particular, the following aspects of porous polymers still need to be further studied: micro scaled thermal radiation, heat transfer characteristics of particular morphologies at the nanoscales, heat transfer mechanism and impact factors of micro/nanoporous polymers. Such studies would provide a more accurate prediction of thermal conductivity and a broader application in energy conversion and storage systems.

Keywords thermal conductivity, micro/nanoscale thermal radiation, micro/nanoscale thermal conduction, porous polymers, heat transfer properties

Contents

1 Introduction

Nowadays, as the increasing fossil fuel continuous depletion [1–3] and global severe environmental problems [4–6], exploring novel energy-saving and environmentally-

* Special Topic: Thermodynamics and Thermal Metamaterials (Editor: Ji-Ping Huang).
arXiv: 2108.02445. This article can also be found at http://journal.hep.com.cn/fop/EN/10.1007/s11467-021-1107-4.

friendly materials become essential for the sustainable development of the economy and society [7–9]. The burgeoning progress of microscale and nanoscale porous polymer materials in recent years has demonstrated that this kind of materials with its low density [10–14], high surface area [15–19] and perfect thermal insulation properties [20–24] for possible challenging social and economic issues. Generally speaking, different materials, processing methods, and environmental conditions also influence the morphologies of porous polymers. Figure 1 represents the SEM images of various micro/nano-porous polymers' morphological characteristics [24–32]. Meanwhile, the morphology of the porous polymers could be divided into open-cell and closed-cell morphologies. Open-cell porous polymers have highly interconnected [Figs. 1(a)–(g)], while closed-cell porous polymers have isolated pores in which the gas is enclosed [Figs. 1(h) and (i)] [33, 34].

Actually, porous polymers are widely used in various burgeoning fields, such as gas capture [35–38], catalysis [39–41], water treatment [42–44], sensors [45–47], molecular separation [48–52], food industry [53–55], proton conduction [56–58], pharmaceutical industry [59–61], drug delivery [62–64], supercapacitors [65–67], synthetic chemistry [68–70], petrochemical engineering [71–73], Li-on batteries [74–76, 78], environmental protection [79–82], and some others [83–91].

In recent years, in order to solve the increasingly severe energy shortage problem, the potential of polymer foam in the field of energy utilization and management system has been dramatically highlighted, such as outer layer of buildings [92–97], photoenergy conversion in solar cells [98–102], electrochemical energy storage [103–108], personal thermal management devices [109–114], and some others [24, 115–119]. Therefore, it is necessary to build an accurate and appropriate thermal conductivity prediction model of micro/nano-porous polymers for better designing and applying its heat transfer characteristics [120–123] in energy conversion and storage systems [124–128], as shown in Fig. 2 [79, 122, 123, 129–133].

This review summarizes the thermal conductivity prediction models of porous polymers, to help subsequent scholars to conveniently carry out their research. Firstly, it reviews the process of establishing the overall equivalent thermal conductivity calculation model for micro/nano porous polymers. Then, the thermal conductivity prediction calculation models are introduced according to thermal conduction and thermal radiation separately. In addition, the thermal conduction part is divided into the gaseous thermal conductivity calculation model, solid thermal conductivity calculation model and gas–solid coupling model. Finally, we conclude and point out the aspects that still need further study of the existing thermal conductivity prediction models of micro/nano porous polymers. Such studies would provide a more accurate prediction of thermal conductivity and a broader application in energy conversion and storage systems.

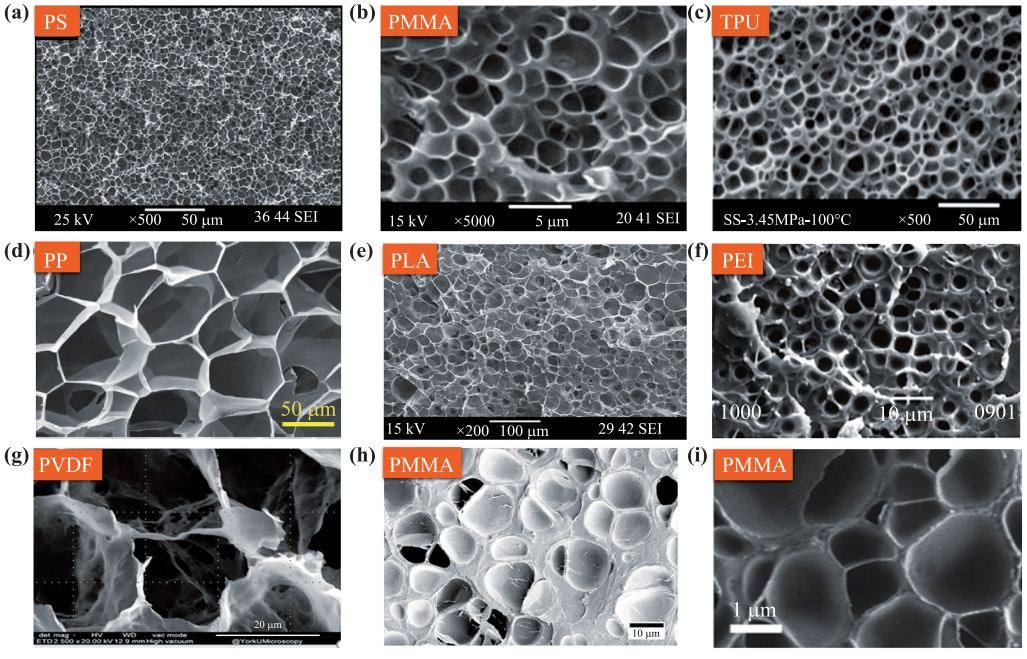

Fig. 1 SEM images of various micro/nano-porous polymeric materials: **(a)** open-cell polystyrene (PS) [25]; **(b)** open-cell poly(methyl methacrylate) (PMMA) [26]; **(c)** open-cell thermoplastic polyurethane (TPU) [27]; **(d)** open-cell polypropylene (PP) [24]; **(e)** open-cell poly(lactic acid) (PLA) [28]; **(f)** open-cell poly(ether imide) (PEI) [29]; **(g)** open-cell poly(vinylidene fluoride) (PVDF) [30]; **(h)** closed-cell PMMA [31]; **(i)** closed-cell PMMA [32].

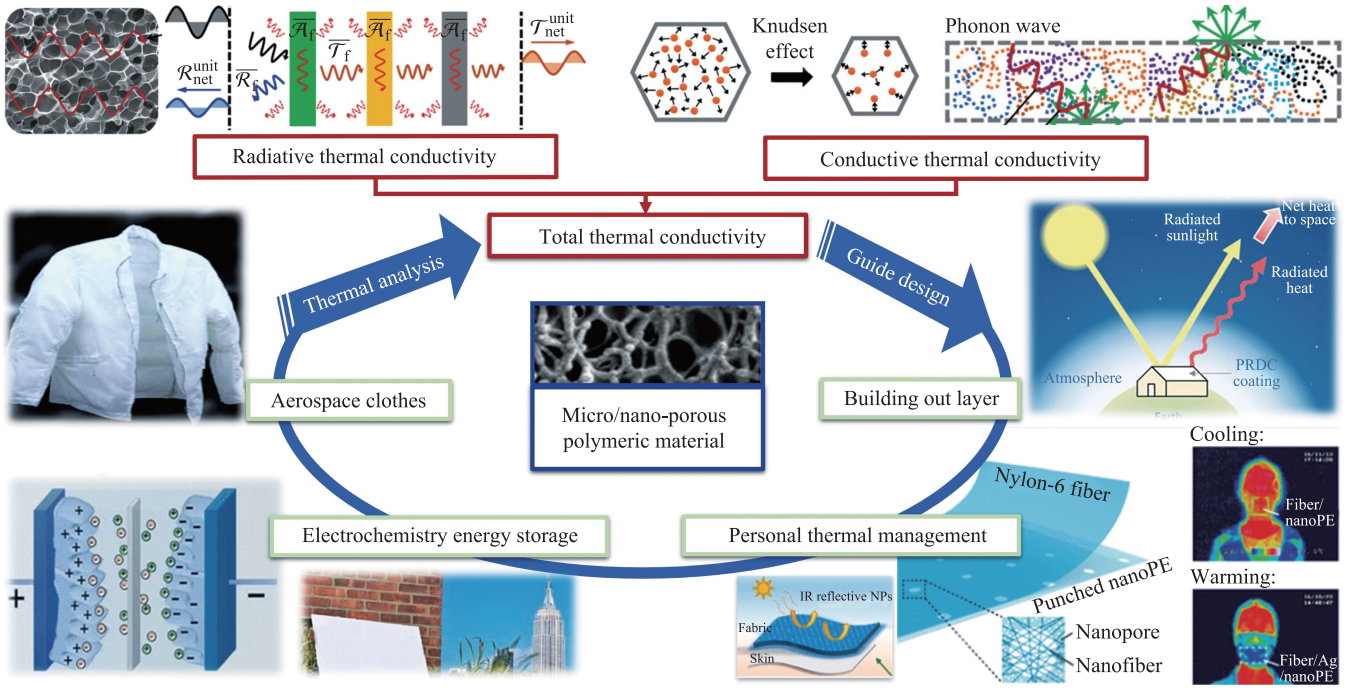

Fig. 2 The schematic diagram of the connection between the thermal conductivity of porous polymeric materials and their potential applications. The figure inserts are produced from references as follows: thermal conductivity figures [122, 123], aerospace cloth figure [129], electrochemistry energy storage figure [130], personal thermal management figures [131, 132] and building out layer figures [79, 133].

2 Overview of the thermal conductivity predicted models

In order to analyze the heat transfer characteristic of the porous polymers, it ought to be noted that thermal convection plays a minor role in closed-pore materials with pore sizes below 4 mm in diameter [22, 33] and in open-pore systems with pore sizes less than 2 mm [25, 134]. Therefore, in microscale and nanoscale, heat transfer of porous polymers is mainly composed of two parts: thermal conduction and thermal radiation, while thermal convection at such a confined scale is negligible [22, 25, 135]. That is, the effective total thermal conductivity of the micro/nano-porous polymers κ_{total} is considered as composed of conductive and radiative components, as [136–

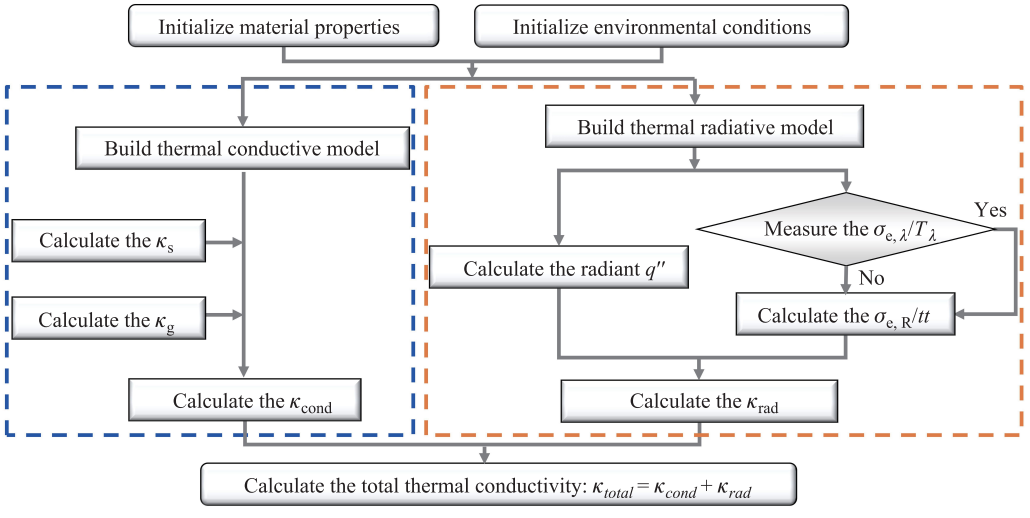

Fig. 3 Flow diagram of the thermal conductivity of micro/nano-porous polymers calculation progress.

139]:

$$\kappa_{total} = \kappa_{cond} + \kappa_{rad}, \tag{1}$$

where the conductive thermal conductivity κ_{cond}, and the radiative thermal conductivity κ_{rad}. To sum up, the overall calculation flow chart is shown in Fig. 3. Next, the prediction models of micro/nano-porous polymers would be discussed from thermal conduction and thermal radiation parts.

2.1 Conductive thermal conductivity models

Generally, while establishing the conductive thermal conductivity models, the gaseous and solid thermal conductivities would be calculated separately by selected predicted models. And then bring the results into the gas–solid coupling model to solve the overall conductive thermal conductivity [14, 22, 25]. Next, these three kinds of predicted models would be introduced separately in the following sections.

2.1.1 Gaseous thermal conductivity models

According to the molecular kinetics theory [140], the gaseous thermal conduction is carried out by the collision of gas molecules during thermal motion [141]. The gas molecules move randomly, and the molecules at the high-temperature side have higher speed collide with molecules at the low-temperature side, causing the energy to be transferred to the lower speed molecules [141, 142].

The gaseous thermal conductivity κ_g inside a micro/nanocellular porous polymer was determined by taking the Knudsen effect [122, 123, 143, 144] into account, which significantly lead to the gaseous thermal conductivity decrease [25, 136]. This Knudsen effect implies that when cell size is comparable or smaller than the mean free path of the liquid or gas, the latter molecules collide more often with the molecules forming the surrounding solid part than among them, reducing the energy transfer through the gas molecules [34, 143]. In a confined space, translation of gas molecules is governed by the Knudsen regime, in which the influence of cell size and mean free path on the efficiency of energy transfer is considered [123, 136, 140],

$$k_g = \frac{k_{g,bulk}}{1+2\beta Kn} = \frac{k_{g,bulk}}{1+2\beta\frac{\Lambda}{d}}, \tag{2}$$

$$2\beta = \frac{2-\alpha_T}{\alpha_T} \cdot \frac{9\gamma-5}{\gamma+1}, \tag{3}$$

where $Kn = \Lambda/d$ is the Knudsen number [145–147], which refers to the ratio of the mean free path Λ of the gas to the cell size d [136]. β is the energy interaction between gaseous molecules and the solid surface [25, 148], which is related to the thermal accommodation coefficient α_T [149, 150] and heat capacity ratio γ [136, 151, 152]. The gaseous thermal conductivities are calculated for different polymer materials considering the Knudsen effect, compared with the experimental data in related reference, shown in Fig. 4 [25, 122, 140, 153].

For the aerogel materials with large porosity and specific surface area, the gaseous thermal conductivity model proposed by Zeng *et al.* [154] also had a wide range of use in the prediction models of aerogel [142, 155, 156], which is simplified as

$$\kappa_g = \frac{60.22 \times pT^{-0.5}}{0.25 S_s \rho \varphi^{-1} + 4.01 \times 10^4 \times pT^{-1}}, \tag{4}$$

where p is pressure, S_s is specific surface area, T is temperature, φ denotes porosity and ρ represents the density of the porous material. Besides, considering the actual pore distribution in porous materials, Reichenauer *et al.* [153] proposed a calculation model for the gas phase thermal conductivity of porous materials based on double pore size distribution as well as the Gauss distribution. Meanwhile, Bi *et al.* [157] proposed a modified gaseous thermal conductivity model considering the randomness and inhomogeneity of pore distribution in aerogel materials.

What's more, Fricke *et al.* [158] fitted the gaseous thermal conductivity of aerogel as a function of material density based on the experimental measurement results of aerogel thermal conductivity, which can be written as

$$\kappa_g \propto \rho^{-0.6}. \tag{5}$$

It should be noted that the above equation is the contribution of the gaseous conductivity obtained directly from the experimental data to the overall thermal conductivity, not the gaseous thermal conductivity inside the pore. However, this empirical formula also needed to be refitted when the materials, densities, and boundary conditions changed.

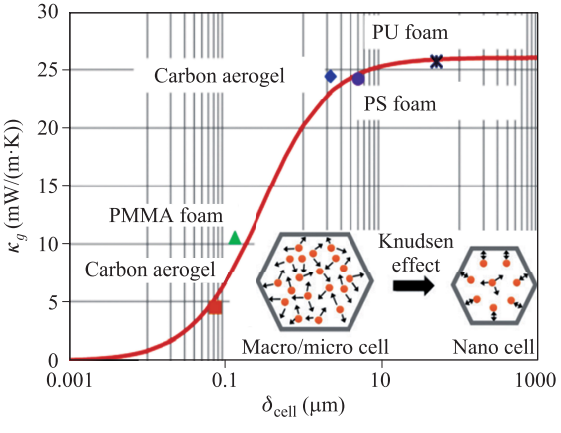

Fig. 4 The size effect on the gaseous thermal conductivities within the cells. The figure inserts are produced from references as follows: Knudsen effect [122], PU foam [153], PS foam [25], Carbon aerogel [153] and PMMA foam [143].

2.1.2 Solid thermal conductivity models

Since the characteristic size of the porous polymer is at the microscale or even nanoscale, which is close to or smaller than the mean free path, leading to a noticeable size effect on the heat transfer progress of the solid framework [140, 141]. As a result, the solid heat transfer of polymer materials is significantly reduced [141].

In some research, the solid thermal conductivity κ_s is theoretically extracted by considering the absence of gas in the porous polymers [25, 136], which is directly equal to the thermal conductivity of the polymer skeleton.

Considering the influence of phonon scattering at the gas–solid interface as seen in Fig. 5, Wang *et al.* [122, 123] gave the thermal conductivity of the thin polymer skeleton based on the kinetic theory [140, 159], as

$$\kappa_s = \left(1 + \frac{\Lambda_s}{\delta}\right)^{-1} \kappa_{bulk}, \tag{6}$$

where κ_{bulk} is the thermal conductivity of pure solid material, δ is the characteristic size of the polymer skeleton. Λ_s is the phonon mean free path of the bulk polymer, which can be calculated based on the thermal conductivity of bulk polymer:

$$\Lambda_s = \frac{3\kappa_{bulk}}{C_v v_g}, \tag{7}$$

where C_v is the specific heat per unit volume contributed by phonons, and v_g is the mean group velocity of phonons [140, 159]. Besides, this kind of modified model, considering the size effect, also wildly used the thermal conductivity calculation of aerogel materials [141, 142, 160]. Therefore, the thermal conductivity of the PS film based on Eq. (6) was calculated with a phonon mean-free path of 1.5 nm, which is in good agreement with those in the literature, as shown in Fig. 5.

Due to the size effect, the polymer film's thermal conductivity reduces significantly with its thickness in the given range [140, 159]. What's more, Fricke *et al.* [157] fitted the solid thermal conductivity of aerogel as a function of material density based on the experimental measurement results of aerogel thermal conductivity, can be written as

$$\kappa_s \propto \rho^{1.5}. \tag{8}$$

It should be noted that this formula also needed to be refitted when the materials, densities, and boundary conditions changed.

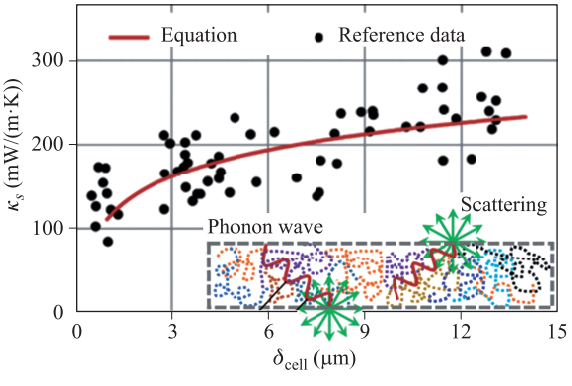

Fig. 5 The size effect on the solid thermal conductivities within the cells. The figure inserts are produced from references as follows: phonon wave scattering [122] and reference data [25].

2.1.3 Gas–solid coupling models

The existing models for the conductive thermal conductivity of porous polymers generally fall into four categories: (i) Empirical model; (ii) Equivalent circuit method; (iii) Equivalent fractal method; (iv) Numerical simulation method. In the following sections, we will introduce the simplified assumptions and application scope of these four methods.

Empirical models. Fricke *et al.* [157] fitted the thermal conductivity of aerogel as a function of material density based on the experimental measurement results. This method is used to adding the contribution values of thermal conductivity, which is simple in form and convenient to handle, as [142, 158]

$$\kappa_{cond} = \kappa_g + \kappa_s. \tag{9}$$

Alshrah *et al.* [161] identified the morphological features in an organic resorcinol-formaldehyde (RF) aerogel. They also correlated each mode of the heat transfer, assuming no coupling effect occurred within the solid–gas phase.

In subsequent studies, some scholars still use this method to calculate aerogel's overall equivalent thermal conductivity, such as Reichenauer *et al.* [153], Lee *et al.* [162], Deng *et al.* [163], Spagnol *et al.* [164], and Swimm *et al.* [165]. In addition, combined with the effective medium method, this empirical method [141, 166, 167] is often used to predict the equivalent thermal conductivity of polymer foam composites doped with carbon and other materials. However, this empirical prediction method usually has several empirical constants with no specific physical meaning in its equation, which is often changed with working conditions [142]. Therefore, this kind of method needs empirical correlation comparing with experimental data each time, which is specifically dependent on the materials' properties and cellular structure.

Equivalent circuit method. Based on Kirchhoff's law, equivalent circuit method simplifies the complex structure into a regularized model and then connects the thermal resistance of each component in series and parallel. In the calculation of conductive thermal conductivity,

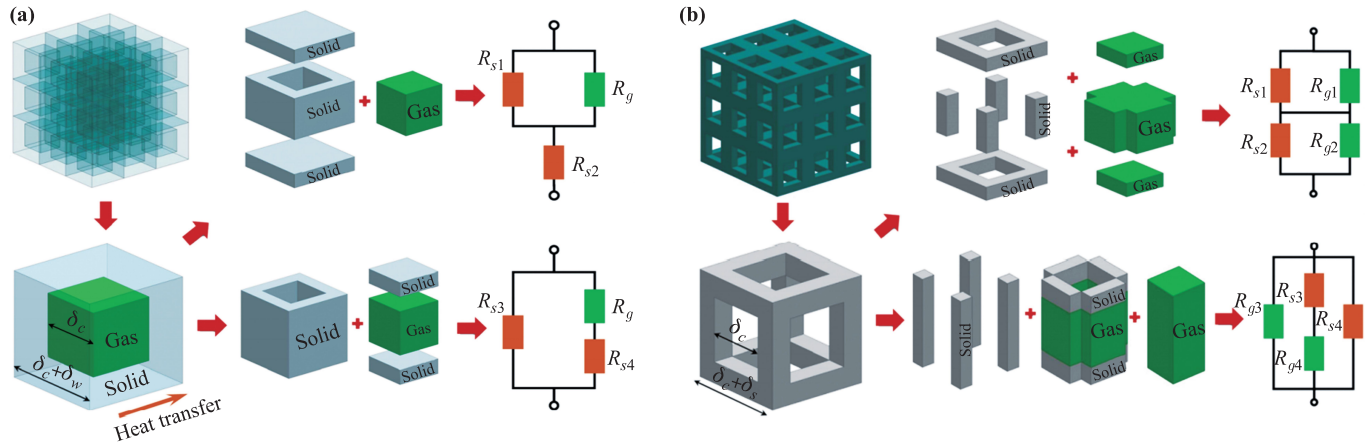

Fig. 6 Schematic diagram of the procedure used for deriving thermal conduction of the foam fully composed with the struts [122, 123]. **(a)** closed-cell model; **(b)** open-cell model.

this method is used as an analytical expression for the conductive thermal conductivity of the entire porous structure, determined by analyzing a network of thermal resistances for an ideal periodic unit consisting of cell struts and/or cell walls [165, 168, 169].

Wang *et al.* [122, 123] proposed the equivalent circuit conductive thermal conductivity models of both closed-cell and open-cell porous polymers, taking the phonon scattering effect into account, as shown in Fig. 6. This method has given mathematical expressions of the conductive thermal conductivity consist of the void fraction (VF), the strut fraction ($\mathrm{F_{strut}}$) and the gas-to-solid thermal conductivity ratio (k_g/k_s). The conductive thermal conductivities of cell walls $k_{c,\mathrm{wall}}$ and struts $k_{c,\mathrm{strut}}$ were determined by analyzing the thermal resistance circuit of heat conduction based on the parallel-series and series-parallel methods for cubic foams [122, 123], as

$$k_{\mathrm{cond}}=(1-F_{\mathrm{strut}})\,k_{c,\mathrm{wall}}+F_{\mathrm{strut}}k_{c,\mathrm{strut}}, \tag{10}$$

$$k_{c,\mathrm{wall}}=\frac{k_{c,\mathrm{wall}}^{(\mathrm{parallel})}+k_{c,\mathrm{wall}}^{(\mathrm{series})}}{2}, \tag{11}$$

$$k_{c,\mathrm{strut}}=\frac{k_{c,\mathrm{strut}}^{(\mathrm{parallel})}+k_{c,\mathrm{strut}}^{(\mathrm{series})}}{2}, \tag{12}$$

where $k_{c,\mathrm{wall}}^{(\mathrm{parallel})}$ and $k_{c,\mathrm{wall}}^{(\mathrm{series})}$ are the conductive thermal conductivities of cell walls based on parallel–series and series–parallel methods, and $k_{c,\mathrm{strut}}^{(\mathrm{parallel})}$ and $k_{c,\mathrm{strut}}^{(\mathrm{series})}$ are the conductive thermal conductivities of struts based on parallel–series and series–parallel methods, respectively [136].

Based on this, Buahom *et al.* [136] introduced a series of alternative mathematical expressions for the conductive thermal conductivity in terms of the void fraction and the gas-to-solid thermal conductivity, as summarized in Table 1. These expressions are derived from those existing expressions based on heat conduction through closed-cell and open-cell foams.

Zeng *et al.* [154] and Wei *et al.* [168] also used equivalent circuit method to calculate the overall conductive thermal conductivity of aerogel materials, while Lu *et al.* [155] used this method to calculate the conductive thermal conductivity of aerogel composite materials.

Table 1 Mathematical expressions of the conductive thermal conductivity models for the parallel–series and series–parallel cell walls and struts [136].

Part	Model	Mathematical expression	
Cell walls	Parallel–Series	$\frac{k_{c,\mathrm{wall}}^{(\mathrm{parallel})}}{k_s}=\frac{1-\left(1-\frac{k_g}{k_s}\right)VF^{2/3}}{1-\left(1-\frac{k_g}{k_s}\right)(VF^{2/3}-VF)}$	(13)
	Series–Parallel	$\frac{k_{c,\mathrm{wall}}^{(\mathrm{series})}}{k_s}=\left(1-VF^{2/3}\right)+\frac{\frac{k_g}{k_s}VF^{2/3}}{\frac{k_g}{k_s}+\left(1-\frac{k_g}{k_s}\right)VF^{1/3}}$	(14)
Struts	Parallel–Series	$\frac{k_{c,\mathrm{strut}}^{(\mathrm{parallel})}}{k_s}=t_{VF}^2+\frac{k_g}{k_s}(1-t_{VF})^2+\frac{2t_{VF}(1-t_{VF})\frac{k_g}{k_s}}{1-t_{VF}\left(1-\frac{k_g}{k_s}\right)}$	(15)
	Series–Parallel	$\frac{k_{c,\mathrm{strut}}^{(\mathrm{series})}}{k_s}=\frac{1}{\frac{1-t_{VF}}{t_{VF}^2\left(1-\frac{k_g}{k_s}\right)+\frac{k_g}{k_s}}+\frac{t_{VF}}{1-(1-t_{VF})^2\left(1-\frac{k_g}{k_s}\right)}}$	(16)

Note: Here $t_{VF}=t_S/d$, which is the ratio of the thickness of rectangular struts in the open-cell cubic foams t_S to the cell size d, can be obtained by solving $2t_{VF}^3-3t_{VF}^2+1-VF=0$.

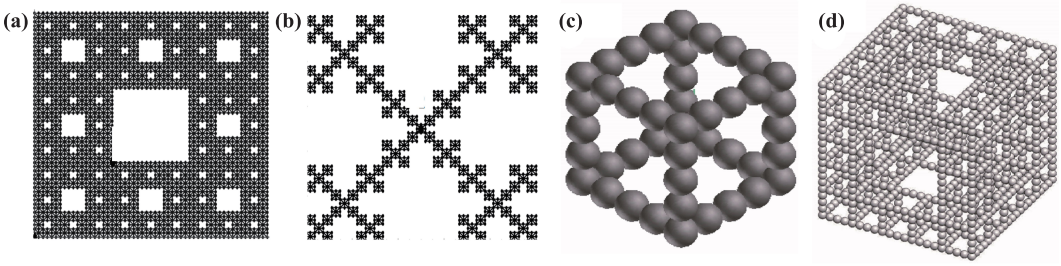

Fig. 7 Fractal heat transfer models: **(a)** Sierpinski carpet [179]; **(b)** Vicsek model [179]; **(c)** first stage Fractal-intersecting sphere model [142]; **(d)** second stage Fractal-intersecting sphere model [142].

Equivalent fractal method. Fractal theory can describe the disordered and random generation process of numerous porous materials at the micro- and nano-scale. These porous materials are different from the Euclidean description of proportional scale [170] but satisfy the fractal characteristics [171] for their self-similarity property [172, 173], which represents it can be simplified the whole process by repeating unit. Based on these, equivalent fractal method is a numerical solution [174, 175] for the conductive thermal conductivity is based on fractal geometry theory [170, 176], which presents a random structure and is independent of the scale.

The heat transfer properties of microscale and nanoscale porous materials were studied based on these dispersed fractal models, such as the Sierpinski gasket model [164, 177, 178], Vicsek model [179, 180], the Von Koch snowflakes model [181, 182], and the fractal-intersecting sphere model [141, 142]. To better represent the structure of the porous polymeric material, the fractal-intersecting sphere model was proposed by Xie *et al.* [141, 142] to calculate the conductive thermal conductivity of aerogel, as shown in Fig. 7.

Combined the equivalent circuit method and geometric of the fractal-intersecting sphere model, the conductive thermal conductivity of the fractal-intersecting model at the first stage κ^1_{cond} and second stage κ^2_{cond} respectively was calculated as follows [141, 142]:

$$\kappa^1_{\text{cond}} = 4\kappa_{\text{unit}}\left(\frac{1-\xi}{2}\right)^2 + \frac{4\kappa_{\text{unit}}\kappa_g\xi(1-\xi)}{2\kappa_g\xi(1-\xi)+2\xi} + \kappa_g\xi^2, \quad (17)$$

$$\kappa^2_{\text{cond}} = 4\kappa^1_{\text{cond}}\left(\frac{1-\xi}{2}\right)^2 + \frac{4\kappa^1_{\text{cond}}\kappa_g\xi(1-\xi)}{2\kappa_g\xi(1-\xi)+2\xi} + \kappa_g\xi^2, \quad (18)$$

where κ_{unit} is the conductive thermal conductivity of the primary size, obtained from [183]

$$\kappa_{\text{unit}} = 4\kappa_s\left(\frac{1-\xi}{2}\right)^2 + \frac{4\kappa_s\kappa_g\xi(1-\xi)}{2\kappa_g\xi(1-\xi)+2\kappa_s\xi} + \kappa_g\xi^2 \quad (19)$$

and $\xi = r/d$ is the aspect ratio of the solid particle radius and the cubic skeleton structure.

Numerical simulation method. Sundarram *et al.* [184] used finite element analysis (FEA) [184–186] and molecular dynamics (MD) [187–190] to study the heat transfer properties of porous polymers (in particular, PMMA and PEI). Moreover, the thermal conductivity was predicted to reduce when the pore size decreased from 1 mm to 1 nm, mainly attributed to the phonon scattering effect in the solid polymer matrix. In these researches, a variety of pore configurations could represent the micro/nanoporous structure observed in polymer foams by FEA method. In contrast, MD method treats individual atoms in the model as point masses that interact via established interatomic potentials [184, 191]. In addition, it has also been widely used to predict physical properties of bulk materials [192–196].

Han *et al.* [197] and Zeng *et al.* [198] used Lattice Boltzmann method (LBM) [199–203] to calculate the overall conductive thermal conductivity of aerogel materials. Meanwhile, the scale effect of structural parameters and the temperature dependence of the thermal conductivity of nanoparticles are also studied using this simulation method.

Although the numerical method is complicated to calculate, it can reflect the influence of various factors on thermal conductivity, and it can also consider the situation of complex structures. However, the calculations in the current literature are still concentrated on the situation of some simple structures [141]. What's more, it should be noted that not to repeat considering the gas–solid interface effect in choosing the solid thermal conductivity model and setting the boundary conditions in gas–solid coupling model.

2.2 Radiative thermal conductivity models

The radiant heat transfer inside the polymer material belongs to medium radiation because the polymer material is participatory media for radiant heat transfer. When incident radiant energy enters the material's interior, the material will absorb, refract, and reflect the radiation energy. Namely, the material has attenuation effects such as absorption or scattering of radiation [141]. Compared to the relatively mature development of the conductive thermal conductivity model, a model for the radiative ther-

mal conductivity of porous polymers is still challenging. The radiative thermal conductivity becomes significant, especially in largely expanded porous dielectric materials having higher porosity [12, 22, 204, 205] and a smaller pore size [122, 206–208]. Several existing approaches for modeling the radiative thermal conductivity are based on different assumptions on the micro- and nanoscales.

2.2.1 Radiative transfer equation approximation

Recently, an accurate model for the radiative thermal conductivity was introduced by solving the equivalent radiant thermal conductivity through the radiative transfer equation (RTE) for simple structures [141, 209, 210].

Assuming that in a participating medium that emits, absorbs, and scattering, at position s, the radiation energy transfer direction Ω, according to the conservation of energy, the governing equation for the transfer of radiant energy in the medium can be derived-the radiation transfer equation, as [211, 212]

$$\frac{\mathrm{d}I_\lambda(s,s)}{\mathrm{d}s} = -(\sigma_{a\lambda}+\sigma_{s\lambda})I_\lambda(s,\boldsymbol{s}) + \sigma_{a\lambda}I_{b\lambda}(s) + \frac{\sigma_{s,\lambda}}{4\pi}\int_{4\pi} I_\lambda(s,\boldsymbol{s})\Phi_\lambda(\boldsymbol{s}_i,\boldsymbol{s})\,\mathrm{d}\Omega_i, \tag{20}$$

where, $I_\lambda(s,s)$ is the spectrum radiation intensity corresponding to space position $\boldsymbol{s}$ and transmission direction $\boldsymbol{s}$, $\sigma_{a\lambda}$ and $\sigma_{s\lambda}$ are the spectrum absorption and scattering coefficients [213, 214] in the medium, respectively, and the sum of the two is the spectrum extinction coefficient $\sigma_{e\lambda}$, $\Phi_\lambda(\boldsymbol{s}_i,\boldsymbol{s})$ is the scattering phase function [215, 216]. The radiation transfer equation is integrodifferential and nonlinear in the three-dimensional radiant heat transfer progress for non-gray materials unless in some simple cases, it is difficult to obtain the exact solution of the equation [14, 141]. Therefore, it is necessary to approximate the differential-integral radiation transfer equation with certain assumptions before solving it [141].

Two-flux approximation method (also called Schuster-Schwarschild approximation) [209, 217, 218] is obtained by simplifying the integral-differential radiation transfer equation into a set of linear differential equations, assuming the radiant intensity uniformly distributed in a specific angle range. However, this method is only accurate through optical thinness media, and this method is not suitable for radiation heat transfer problems with strong anisotropic scattering [141].

For the radiation intensity can be divided into several discrete directions in the entire space, Chandrasekhar [219] developed the two-flux approximation by solving the radiation intensity in these discrete directions, known as the discrete-ordinates method [220]. Besides these methods, there are different approximate methods to solve the radiative transfer equation, such as the finite volume method [221–225], discrete transfer method [226, 227], etc.

2.2.2 Ignore some physical processes

When the absorption or scattering of the material is unapparent, and the related term in radiation transfer equation (20) can be ignored [141]. Likewise, the influence of the radiation term is well known in conventional and microporous materials, and this term is negligible for low density foams (<0.2 relative densities) [34, 228]. However, the conventional models used to evaluate the radiation mechanism in porous polymers assumes that the wavelength of the infrared radiation is smaller than the pore size. It should note that this presumption is incorrect in nanoporous polymers [34, 228].

2.2.3 Rosseland diffusion approximation

The diffusion approximation, known as the Rosseland diffusion approximation [209, 230], is well established for optically thick media, which is widely used to calculate the radiative thermal conductivity of porous polymers. If the medium is optically thick, the medium has a strong attenuation effect on radiation, and the transmission distance of radiant energy is very short [209]. Moreover, the radiation transfer equation can be simplified based on this assumption [209].

The radiative thermal conductivity k_{rad} at a mean temperature T_m is usually determined by the corresponding temperature-dependent Rosseland diffusion equation [209, 230], as

$$k_{rad}=\frac{16\sigma_{SB}T_m^3}{3\beta_R}, \tag{21}$$

where σ_{SB} is the Stefan–Boltzmann constant (5.670367 $\times10^{-8}$ W·m^{-2}·K^{-4}) and β_R is the Rosseland mean extinction coefficient of the foam, which indicates attenuation of the radiative energy. β_R is a harmonic mean of the spectral extinction coefficient $\beta_{\lambda,\mathrm{foam}}$ weighted by the temperature derivative of the blackbody spectral intensity for all wavelengths within Planck's blackbody emission spectrum [231, 232], as

$$\frac{1}{\beta_R}=\frac{\int_0^\infty \frac{1}{\beta_{\lambda,\mathrm{foam}}} f_\lambda(\lambda,T)\,\mathrm{d}\lambda}{\int_0^\infty f_\lambda(\lambda,T)\,\mathrm{d}\lambda}, \tag{22}$$

where $f_\lambda(\lambda,\ T)$ is the spectral distribution of Planck's law of blackbody emission. It indicates the fraction of the radiative energy at a wavelength λ to the overall energy over the wavelength spectrum [122, 140], as

$$f_\lambda(\lambda,T)=\frac{\partial e_{b,\lambda}}{\partial \mathrm{T}}=\frac{C_1}{\lambda^5\exp\left(\frac{C_2}{\lambda T}-1\right)}, \tag{23}$$

where $e_{b,\lambda}$ is the blackbody spectral intensity at a wavelength λ. Two auxiliary constants are defined as $C_1 = 2\pi hc^2$ and $C_2 = hc/k_B$. c is the speed of light in vacuum (2.99792458 $\times10^8$ m·s^{-1}). h is the Planck constant (6.62607015 $\times10^{-34}$ J·s) and k_B is the Boltzmann constant (1.380649 $\times10^{-23}$ J·K^{-1}) [209, 233].

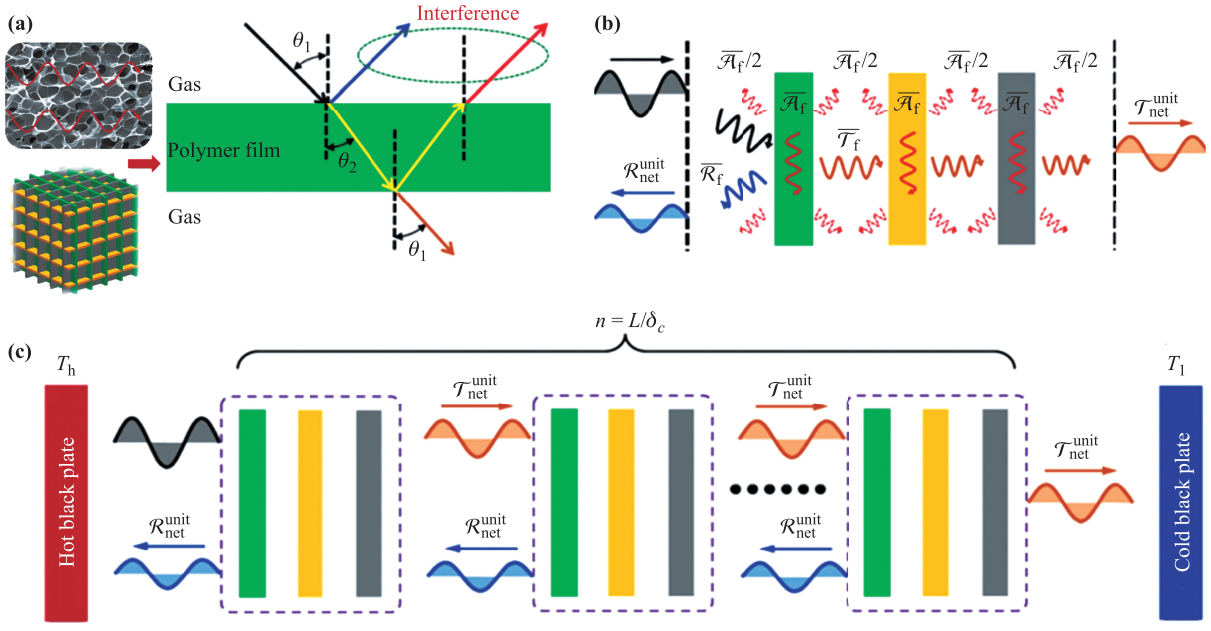

Fig. 8 Schematic diagrams of the thermal radiation wave propagation behaviour through a material that has multiple layers. **(a)** The case of a single polymer film. As the polymer film thickness is much less than the radiation wavelength, the strong thin-film interference effect can significantly reduce the reflectance. **(b)** The single three-slab unit is composed of a reflecting and absorbing slab, and two pure absorbing slabs. Half of the whole absorbed radiant energy will be reemitted backward and the other half will be reemitted forward. **(c)** The case of a set of n three-slab units sandwiched between a hot black plate and a cold black plate [122].

As shown in Fig. 3, $\beta_{\lambda,\mathrm{foam}}$ can be measured by experiments [232] or calculated by Mie theory [234, 235]. Accordingly, the fraction of the radiative energy reflected, absorbed and transmitted at a wavelength λ in the radiation spectrum can be defined as the spectral reflectivity (A_λ), spectral absorptivity (R_λ) and spectral transmissivity (T_λ) of cell wall, respectively. Because $A_{\lambda,\mathrm{wall}}+R_{\lambda,\mathrm{wall}}+T_{\lambda,\mathrm{wall}}=1$, the radiative thermal conductivity could be obtained by measuring or calculating the transmissivity T_λ, as shown in Fig. 3. Therefore, Gong *et al.* [22, 25] used the transmissivity to derive the radiative thermal conductivity formula of the porous polymers. Furthermore, Wang *et al.* [122, 123] considered the interference of the micro/nano-porous polymers' electromagnetic waves and modified the radiative thermal conductivity formula based on the transmissivity formula, as shown in Fig. 8. This method takes the size effect into account, leading to a more accurate thermal radiation prediction especially in the micro/nano-porous polymers. The detail of this microscale radiation method would be exhaustively introduced in the following section.

2.2.4 *Microscale radiation method*

Since Chen *et al.* [236, 237] found that the radiant energy of two very closely located objects is much larger than that predicted by the Planck Stefan–Boltzman law [237, 238], the thermal radiation process needs to consider microscale effect [239, 240]. Maxwell's equations describe the propagation of electromagnetic waves and their interactions with matter [160, 241]. Furthermore, the fluctuational electrodynamics combining the fluctuation-dissipation theorem with Maxwell's equations [140, 242, 243] fully describe thermal radiation's emission, propagation, and absorption in both the near and far fields [211, 244, 245].

Buahom *et al.* [136] determined the radiative thermal conductivity by analyzing the attenuation of radiative energy by absorption and scattering based on Mie's theory, as well as interference of propagating waves and tunneling of evanescent waves in the radiative energy.

This method illustrates that, in the porous polymer, radiation in the form of electromagnetic waves propagates in space and interacts with gas and polymer molecules [136]. Each photon carries a single discrete quantum of thermal radiation and affects the electrons in the material molecule to increase its energy level [136]. Then some of these excited electrons release the electron's excess energy and emit photons in the wavelength range according to Planck's law of blackbody emission [136, 209]. At the same time, multiple internal scattering, absorption, and re-emission occur in the porous polymer, resulting in tortuous transmission paths for radiant energy transfer, especially in such a complex structure, leading to a tortious transport path of radiative energy transfer [22, 136, 209].

As shown in Eq. (22), $\beta_{\lambda,\mathrm{foam}}$ can be obtained by assuming randomly oriented concave-triangular struts and cell walls independently as [136]

$$\beta_{\lambda,\,\mathrm{foam}}=F_{\mathrm{strut}}\beta^{(\mathrm{eff})}_{\lambda,\mathrm{strut}}+(1-F_{\mathrm{strut}})\,\beta^{(\mathrm{eff})}_{\lambda,\mathrm{wall}}, \tag{24}$$

where $\beta_{\lambda,\text{strut}}^{(\text{eff})}$ is the contribution of struts and $\beta_{\lambda,\text{wall}}^{(\text{eff})}$ is the contribution of cell walls, the volume fraction of polymer located in struts, the strut fraction F_{strut}, is used as the weighted factor in the calculation. The effective spectral extinction coefficient of cell wall $\beta_{\lambda,\text{wall}}^{(\text{eff})}$ can be calculated as [136]

$$\beta_{\lambda,\text{wall}}^{(\text{eff})} = N_{v,\text{wall}} C_{\text{wall}}^{(\text{geo})} \int_0^{\frac{\pi}{2}} (1+R_{\lambda,\text{wall}}-T_{\lambda,\text{wall}}) \cdot \frac{\sin(2\phi_1)}{4} \mathrm{d}\phi_1, \tag{25}$$

where $N_{v,\text{wall}}$ is the number of cell walls per unit volume of foam, $C_{\text{wall}}^{(\text{geo})} = C_{\lambda,\text{wall}}^{(\text{ext})}/Q_{\lambda}^{(\text{ext})}$, $C_{\lambda,\text{wall}}^{(\text{ext})}$ is the spectral extinction cross-section of cell wall for the incident beam interacts with a wall tilted by the incident angle ϕ_1. the spectral extinction efficiency factor, the ratio of the spectral extinction cross-section to the geometric cross-section of cell wall at normal incident $Q_{\lambda,\text{wall}}^{(\text{ext})} = R_{\lambda,\text{wall}} + \frac{1}{2}A_{\lambda,\text{wall}}$. Based on Fresnel formula, R_λ and T_λ in Eq. (25) can be written as [246]

$$R_{\lambda,\text{wall}} = \frac{\rho_{\lambda,\text{gs}}^2 + \rho_{\lambda,\text{sg}}^2 + 2\rho_{\lambda,\text{gs}}\rho_{\lambda,\text{sg}}\cos 2\tilde{\beta}_\lambda}{1+\rho_{\lambda,\text{gs}}^2\rho_{\lambda,\text{sg}}^2 + 2\rho_{\lambda,\text{gs}}\rho_{\lambda,\text{sg}}\cos 2\tilde{\beta}_\lambda} \quad \text{and}$$

$$T_{\lambda,\text{wall}} = \frac{\tau_{\lambda,\text{gs}}^2\tau_{\lambda,\text{sg}}^2}{1+\rho_{\lambda,\text{gs}}^2\rho_{\lambda,\text{sg}}^2 + 2\rho_{\lambda,\text{gs}}\rho_{\lambda,\text{sg}}\cos 2\tilde{\beta}_\lambda}, \tag{26}$$

where the spectral reflection and transmission coefficients at the gas–solid ($\rho_{\lambda,\text{gs}}$, $\tau_{\lambda,\text{gs}}$) and solid-gas ($\rho_{\lambda,\text{sg}}$, $\tau_{\lambda,\text{sg}}$) interfaces are defined as [246]

$$\rho_{\lambda,\text{gs}} = -\rho_{\lambda,\text{gs}} = \frac{\hat{n}_{\lambda,\text{g}}\cos\phi_1 - \hat{n}_{\lambda,\text{s}}\cos\phi_2}{\hat{n}_{\lambda,\text{g}}\cos\phi_1 + \hat{n}_{\lambda,\text{s}}\cos\phi_2}, \tag{27}$$

$$\tau_{\lambda,\text{gs}} = \frac{2\hat{n}_{\lambda,\text{g}}\cos\phi_1}{\hat{n}_{\lambda,\text{g}}\cos\phi_1 + \hat{n}_{\lambda,\text{s}}\cos\phi_2}, \quad \text{and}$$

$$\tau_{\lambda,\text{sg}} = \frac{2\hat{n}_{\lambda,\text{s}}\cos\phi_2}{\hat{n}_{\lambda,\text{g}}\cos\phi_1 + \hat{n}_{\lambda,\text{s}}\cos\phi_2}, \tag{28}$$

where $\hat{n}_{\lambda,\text{s}} = n_{\lambda,\text{s}} + \mathrm{i}\kappa_{\lambda,\text{s}}$ and $\hat{n}_{\lambda,\text{g}} = n_{\lambda,\text{g}}$ are the spectral complex refractive indices of polymer film and non-absorbing gas.

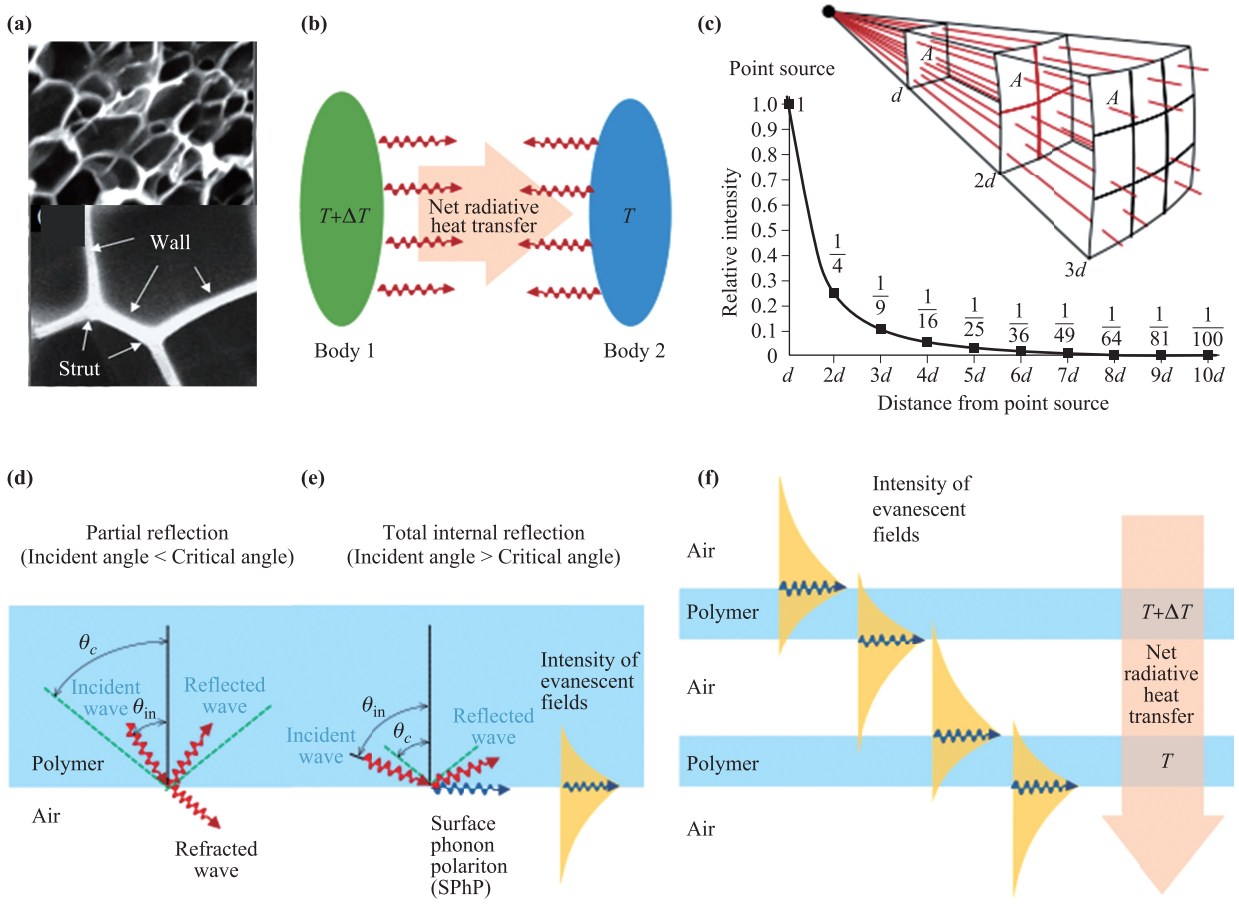

Fig. 9 **(a)** Cell walls and struts in porous polymers morphology; **(b)** energy exchange between an emitter and a receiver; **(c)** the intensity of radiation decreases exponentially with square of the distance from the surface due to an increase in the surface area; **(d)** reflection and refraction of propagating waves in partial reflection; **(e)** surface phonon polaritons in polymers during total internal reflection and the intensity profile of evanescent fields; **(f)** tunneling of radiative energy through the foam structure by evanescent waves [136].

The spectral extinction coefficient of the strut can be expressed in the number density of struts and the geometric cross-section [136]:

$$\beta_{\lambda,\mathrm{strut}}^{(\mathrm{eff})} = N_{v,\mathrm{strut}} C_{\mathrm{strut}}^{(\mathrm{geo})} \int_0^{\frac{\pi}{2}} \left[\left(Q_{\lambda,\mathrm{strut}}^{(\mathrm{ext})} - Q_{\lambda,\mathrm{strut}}^{(\mathrm{sca})} \right) \sin^2\phi - g_{\lambda,\mathrm{strut}} Q_{\lambda,\mathrm{strut}}^{(\mathrm{sca})} \cos^2\phi \right] \cos\phi \mathrm{d}\phi, \quad (29)$$

where $N_{v,\mathrm{strut}}$ is the number of struts per unit volume of porous polymers, which is dependent on the porosity, the cell size, and the strut fraction. $C_{\mathrm{strut}}^{(\mathrm{geo})}$ is the normally projected geometric cross-section of a strut. $g_{\lambda,\mathrm{strut}}$ is the asymmetry factor of the strut. $Q_{\lambda,\mathrm{strut}}^{(\mathrm{sca})}$ and $Q_{\lambda,\mathrm{strut}}^{(\mathrm{ext})}$ are spectral scattering and extinction efficiency factors of the strut, separately split into the TM and TE incident modes [136].

3 Summary and prospects

In this study, the existing thermal conductivity calculation models of micro/nano-porous polymers are introduced and reviewed. Firstly, it reviews the process of establishing the overall equivalent thermal conductivity calculation model for micro/nano-porous polymers. Then, the thermal conductivity prediction model is introduced separately based on thermal conduction and thermal radiation. In addition, the thermal conduction part is divided into the gaseous thermal conductivity calculation model, solid thermal conductivity calculation model and gas–solid coupling model. Finally, it is concluded that, compared with other porous materials, there are few studies on heat transfer of micro/nano-porous polymers, especially on the particular heat transfer mechanisms such as scale effects at the micro/nanoscale. In particular, the following aspects of porous polymers still need to be further studied:

(i) The study of characteristics and influences in micro/nano-porous polymers brought by microscale thermal radiation.

(ii) The research of the heat transfer characteristics of open/ closed-pores and particular morphologies at the nanoscale.

(iii) Heat transfer mechanism and impact factors of micro/nano-porous polymers. By analyzing the various influencing factors on heat transfer performance, the porous polymers can be further optimized for efficient thermal insulation materials, which are well used in energy conversion and storage systems.

Acknowledgements The authors are grateful to the National Natural Science Foundation of China (Nos. 51776050 and 51536001).

References and notes

1. J. Wu, F. Xu, S. Li, P. Ma, X. Zhang, Q. Liu, R. Fu, and D. Wu, Porous polymers as multifunctional material platforms toward task-specific applications, *Adv. Mater.* 31, 4 (2019)
2. B. H. Kreps, Energy sprawl in the renewable-energy sector: moving to sufficiency in a post-growth era, *Am. J. Econ. Sociol.* 79, 3 (2020)
3. S. K. Mangla, S. Luthra, S. Jakhar, S. Gandhi, K. Muduli, and A. Kumar, A step to clean energy — Sustainability in energy system management in an emerging economy context, *J. Clean. Prod.* 242, 118462 (2020)
4. X. Chang, Y. Xue, J. Li, L. Zou, and M. Tang, Potential health impact of environmental micro- and nanoplastics pollution, *J. Appl. Toxicol.* 40(1), 4 (2020)
5. F. A. Faize and M. Akhtar, Addressing environmental knowledge and environmental attitude in undergraduate students through scientific argumentation, *J. Clean. Prod.* 252, 119928 (2020)
6. S. Chu and A. Majumdar, Opportunities and challenges for a sustainable energy future, *Nature* 488(7411), 294 (2012)
7. L. Song, C. Jiang, S. Liu, C. Jiao, X. Si, S. Wang, F. Li, J. Zhang, L. Sun, F. Xu, and F. Huang, Progress in improving thermodynamics and kinetics of new hydrogen storage materials, *Front. Phys.* 6(2), 151 (2011)
8. Z. C. Tu, Abstract models for heat engines, *Front. Phys.* 16(3), 33202 (2021)
9. X. He, A review of material development in the field of carbon capture and the application of membrane-based processes in power plants and energy-intensive industries, *Energy Sustain. Soc.* 8(1), 34 (2018)
10. Y. Huang and X. Feng, Polymer-enhanced ultrafiltration: Fundamentals, applications and recent developments, *J. Membr. Sci.* 586, 53 (2019)
11. S. Wang, Y. Huang, C. Zhao, E. Chang, A. Ameli, H. E. Naguib, and C. B. Park, Theoretical modeling and experimental verification of percolation threshold with MWCNTs' rotation and translation around a growing bubble in conductive polymer composite foams, *Compos. Sci. Technol.* 199, 108345 (2020)
12. M. Hamidinejad, B. Zhao, R. K. M. Chu, N. Moghimian, H. E. Naguib, T. Filleter, and C. B. Park, Enhanced electrical and electromagnetic interference shielding properties of polymer–graphene nanoplatelet composites fabricated via supercritical-fluid treatment and physical foaming, *ACS Appl. Mater. Interfaces* 10, 36 (2018)
13. Y. Huang, T. Gancheva, B. D. Favis, A. Abidli, J. Wang, and C. B. Park, Hydrophobic porous polypropylene with hierarchical structures for ultrafast and highly selective oil/water separation, *ACS Appl. Mater. Interfaces* 13, 14 (2021)
14. J. Zhao, G. Wang, Z. Chen, Y. Huang, C. Wang, A. Zhang, and C. B. Park, Microcellular injection molded outstanding oleophilic and sound-insulating PP/PTFE nanocomposite foam, *Compos. Part B Eng.* 215, 108786 (2021)

15. B. Zhao, M. Hamidinejad, C. Zhao, R. Li, S. Wang, Y. Kazemi, and C. B. Park, A versatile foaming platform to fabricate polymer/carbon composites with high dielectric permittivity and ultra-low dielectric loss, *J. Mater. Chem. A* 7(1), 133 (2019)
16. J. Zhao, G. Wang, L. Zhang, B. Li, C. Wang, G. Zhao, and C. B. Park, Lightweight and strong fibrillary PTFE reinforced polypropylene composite foams fabricated by foam injection molding, *Eur. Polym. J.* 119, 22 (2019)
17. J. M. Eagan, J. Xu, R. Di Girolamo, C. M. Thurber, C. W. Macosko, A. M. La Pointe, F. S. Bates, and G. W. Coates, Combining polyethylene and polypropylene: Enhanced performance with PE/*i*PP multiblock polymers, *Science* 355(6327), 814 (2017)
18. Z. Zhang, W. Li, and J. Kan, Behavior of a thermoelectric power generation device based on solar irradiation and the earth's surface-air temperature difference, *Energy Convers. Manage.* 97, 178 (2015)
19. S. A. Khan, N. Sezer, S. Ismail, and M. Koç, Design, synthesis and nucleate boiling performance assessment of hybrid micro-nano porous surfaces for thermal management of concentrated photovoltaics (CPV), *Energy Convers. Manage.* 195, 1056 (2019)
20. J. Zhao, Y. Huang, G. Wang, Y. Qiao, Z. Chen, A. Zhang, and C. B. Park, Fabrication of outstanding thermal-insulating, mechanical robust and superhydrophobic PP/CNT/sorbitol derivative nanocomposite foams for efficient oil/water separation, *J. Hazard. Mater.* 418, 126295 (2021)
21. J. Zhao, Q. Zhao, L. Wang, C. Wang, B. Guo, C. B. Park, and G. Wang, Development of high thermal insulation and compressive strength BPP foams using mold-opening foam injection molding with in-situ fibrillated PTFE fibers, *Eur. Polym. J.* 98, 1 (2018)
22. P. Gong, G. Wang, M. P. Tran, P. Buahom, S. Zhai, G. Li, and C. B. Park, Advanced bimodal polystyrene/multi-walled carbon nanotube nanocomposite foams for thermal insulation, *Carbon* 120, 1 (2017)
23. G. Wang, J. Zhao, G. Wang, H. Zhao, J. Lin, G. Zhao, and C. B. Park, Strong and super thermally insulating in-situ nanofibrillar PLA/PET composite foam fabricated by high-pressure microcellular injection molding, *Chem. Eng. J.* 390, 124520 (2020)
24. J. Zhao, G. Wang, C. Wang, and C. B. Park, Ultra-lightweight, super thermal-insulation and strong PP/CNT microcellular foams, *Compos. Sci. Technol.* 191, 108084 (2020)
25. P. Gong, P. Buahom, M. P. Tran, M. Saniei, C. B. Park, and P. Pötschke, Heat transfer in microcellular polystyrene/multi-walled carbon nanotube nanocomposite foams, *Carbon* 93, 819 (2015)
26. G. Wang, J. Zhao, L. H. Mark, G. Wang, K. Yu, C. Wang, C. B. Park, and G. Zhao, Ultra-tough and super thermal-insulation nanocellular PMMA/TPU, *Chem. Eng. J.* 325, 632 (2017)
27. G. Wang, J. Zhao, K. Yu, L. H. Mark, G. Wang, P. Gong, C. B. Park, and G. Zhao, Role of elastic strain energy in cell nucleation of polymer foaming and its application for fabricating sub-microcellular TPU microfilms, *Polymer (Guildf.)* 119, 28 (2017)
28. L. Wang, R. E. Lee, G. Wang, R. K. M. Chu, J. Zhao, and C. B. Park, Use of stereocomplex crystallites for fully-biobased microcellular low-density poly(lactic acid) foams for green packaging, *Chem. Eng. J.* 327, 1151 (2017)
29. B. Krause, H. J. P. Sijbesma, P. Münüklü, N. F. A. Van Der Vegt, and M. Wessling, Bicontinuous nanoporous polymers by carbon dioxide foaming, *Macromolecules* 34, 25 (2001)
30. S. N. Leung, and J. E. Lee, Tunable microcellular and nanocellular morphologies of poly(vinylidene) fluoride foams via crystal polymorphism control, *Polymer Crystallization* 2(1), 1 (2019)
31. S. Pérez-Tamarit, B. Notario, E. Solórzano, and M. A. Rodriguez-Perez, Light transmission in nanocellular polymers: Are semi-transparent cellular polymers possible? *Mater. Lett.* 210, 39 (2018)
32. S. Liu, R. Eijkelenkamp, J. Duvigneau, and G. J. Vancso, Silica-assisted nucleation of polymer foam cells with nanoscopic dimensions: impact of particle size, line tension, and surface functionality, *ACS Appl. Mater. Interfaces* 9, 43 (2017)
33. B. Notario, J. Pinto, and M. A. Rodriguez-Perez, Nanoporous polymeric materials: A new class of materials with enhanced properties, *Prog. Mater. Sci.* 78–79, 93 (2016)
34. B. Notario, J. Pinto, and M. A. Rodríguez-Pérez, Towards a new generation of polymeric foams: PMMA nanocellular foams with enhanced physical properties, *Polymer (Guildf.)* 63, 116 (2015)
35. Y. Zeng, R. Zou, and Y. Zhao, Carbon dioxide capture: Covalent organic frameworks for CO_2 capture, *Adv. Mater.* 28, 3032 (2016)
36. L. Zou, Y. Sun, S. Che, X. Yang, X. Wang, M. Bosch, Q. Wang, H. Li, M. Smith, S. Yuan, Z. Perry, and H. C. Zhou, Porous organic polymers for post-combustion carbon capture, *Adv. Mater.* 29, 37 (2017)
37. X. Liu, G. J. H. Lim, Y. Wang, L. Zhang, D. Mullangi, Y. Wu, D. Zhao, J. Ding, A. K. Cheetham, and J. Wang, Binder-free 3D printing of covalent organic framework (COF) monoliths for CO_2 adsorption, *Chem. Eng. J.* 403, 126333 (2021)
38. M. Wang, S. Zhou, S. Cao, Z. Wang, S. Liu, S. Wei, Y. Chen, and X. Lu, Stimulus-responsive adsorbent materials for CO_2 capture and separation, *J. Mater. Chem. A* 8, 10519 (2020)
39. P. Puthiaraj, Y. R. Lee, S. Zhang, and W. S. Ahn, Triazine-based covalent organic polymers: design, synthesis and applications in heterogeneous catalysis, *J. Mater. Chem. A* 4(42), 16288 (2016)
40. Y. Zhang and S. N. Riduan, Functional porous organic polymers for heterogeneous catalysis, *Chem. Soc. Rev.* 41, 6 (2012)
41. Z. Ma, J. Zhuang, X. Zhang, and Z. Zhou, SiP monolayers: New 2D structures of group IV–V compounds for visible-light photohydrolytic catalysts, *Front. Phys.* 13(3), 138104 (2018)

42. M. Kilpatrick, R. D. Eanes, and J. G. Morse, The dissociation constants of acids in salt solutions(IV): Cyclohexanecarboxylic acid, *J. Am. Chem. Soc.* 75(3), 588 (1953)
43. A. Chakrabarti and M. M. Sharma, Cationic ion exchange resins as catalyst, *Reactive Polymers* 20(1–2), 1 (1993)
44. R. Liu, Z. Yang, S. Chen, J. Yao, Q. Mu, D. Peng, and H. Zhao, Synthesis and facile functionalization of siloxane based hyper-cross-linked porous polymers and their applications in water treatment, *Eur. Polym. J.* 119, 94 (2019)
45. C. Gu, N. Huang, J. Gao, F. Xu, Y. Xu, and D. Jiang, Controlled synthesis of conjugated microporous polymer films: Versatile platforms for highly sensitive and label — free chemo — and biosensing, *Angew. Chem.* 126(19), 4950 (2014)
46. S. Luo, Z. Zeng, G. Zeng, Z. Liu, R. Xiao, P. Xu, H. Wang, D. Huang, Y. Liu, B. Shao, Q. Liang, D. Wang, Q. He, L. Qin, and Y. Fu, Recent advances in conjugated microporous polymers for photocatalysis: Designs, applications, and prospects, *J. Mater. Chem. A* 8(14), 6434 (2020)
47. Y. N. Jiang, J. H. Zeng, Y. Yang, Z. K. Liu, J. J. Chen, D. C. Li, L. Chen, and Z. P. Zhan, A conjugated microporous polymer as a recyclable heterogeneous ligand for highly efficient regioselective hydrosilylation of allenes, *Chem. Commun.* 56(10), 1597 (2020)
48. S. Kim and Y. M. Lee, Rigid and microporous polymers for gas separation membranes, *Prog. Polym. Sci.* 43, 1 (2015)
49. A. I. Cooper, Conjugated microporous polymers, *Adv. Mater.* 21(12), 1291 (2009)
50. F. Vilela, K. Zhang, and M. Antonietti, Conjugated porous polymers for energy applications, *Energy Environ. Sci.* 5(7), 7819 (2012)
51. J. Pinto, A. Athanassiou, and D. Fragouli, Surface modification of polymeric foams for oil spills remediation, *J. Environ. Manage.* 206, 872 (2018)
52. O. Oribayo, X. Feng, G. L. Rempel, and Q. Pan, Modification of formaldehyde-melamine-sodium bisulfite copolymer foam and its application as effective sorbents for clean up of oil spills, *Chem. Eng. Sci.* 160, 384 (2017)
53. M. R. El-Aassar, M. S. Masoud, M. F. Elkady, and A. A. Elzain, Synthesis, optimization, and characterization of poly (Styrene-co-Acrylonitrile) copolymer prepared via precipitation polymerization, *Adv. Polym. Technol.* 37(6), 2021 (2018)
54. A. Akelah, Functionalized Polymeric Materials in Agriculture and the Food Industry, Springer US, 2013
55. M. Noruzi, Electrospun nanofibres in agriculture and the food industry: A review, *J. Sci. Food Agric.* 96(14), 4663 (2016)
56. X. Meng, H. N. Wang, S. Y. Song, and H. J. Zhang, Proton-conducting crystalline porous materials, *Chem. Soc. Rev.* 46(2), 464 (2017)
57. S. Horike, D. Umeyama, and S. Kitagawa, Ion conductivity and transport by porous coordination polymers and metal–organic frameworks, *Acc. Chem. Res.* 46(11), 2376 (2013)
58. H. Xu, S. Tao, and D. Jiang, Proton conduction in crystalline and porous covalent organic frameworks, *Nat. Mater.* 15(7), 722 (2016)
59. P. M. Valetsky, M. G. Sulman, L. M. Bronstein, E. M. Sulman, A. I. Sidorov, and V. G. Matveeva, Nanosized catalysts in fine organic synthesis as a basis for developing innovative technologies in the pharmaceutical industry, *Nanotechnol. Russ.* 4(9–10), 647 (2009)
60. M. Sauceau, J. Fages, A. Common, C. Nikitine, and E. Rodier, New challenges in polymer foaming: A review of extrusion processes assisted by supercritical carbon dioxide, *Prog. Polym. Sci.* 36(6), 749 (2011)
61. J. Shokri and K. Adibki, in: Cellulose — Medical, Pharmaceutical and Electronic Applications, InTech, 2013
62. Q. Fang, J. Wang, S. Gu, R. B. Kaspar, Z. Zhuang, J. Zheng, H. Guo, S. Qiu, and Y. Yan, 3D porous crystalline polyimide covalent organic frameworks for drug delivery, *J. Am. Chem. Soc.* 137(26), 8352 (2015)
63. L. Feng, C. Qian, and Y. Zhao, Recent advances in covalent organic framework-based nanosystems for bioimaging and therapeutic applications, *ACS Mater. Lett.* 2, 1074 (2020)
64. M. C. Scicluna and L. Vella-Zarb, Evolution of nanocarrier drug-delivery systems and recent advancements in covalent organic framework–drug systems, *ACS Appl. Nano Mater.* 3(4), 3097 (2020)
65. N. Yadav, K. Mishra, and S. A. Hashmi, Optimization of porous polymer electrolyte for quasi-solid-state electrical double layer supercapacitor, *Electrochim. Acta* 235, 570 (2017)
66. R. C. Agrawal, and G. P. Pandey, Solid polymer electrolytes: Materials designing and all-solid-state battery applications: an overview, *J. Phys. D Appl. Phys.* 41(22), 223001 (2008)
67. D. T. Jr Hallinan and N. P. Balsara, Polymer electrolytes, *Annu. Rev. Mater. Res.* 43(1), 503 (2013)
68. S. Kramer, N. R. Bennedsen, and S. Kegnæs, Porous organic polymers containing active metal centers as catalysts for synthetic organic chemistry, *ACS Catal.* 8(8), 6961 (2018)
69. I. Ro, J. Resasco, and P. Christopher, Approaches for understanding and controlling interfacial effects in oxide-supported metal catalysts, *ACS Catal.* 8(8), 7368 (2018)
70. S. H. Xie, Y. Y. Liu, and J. Y. Li, Synthesis, microstructures, and magnetoelectric couplings of electrospun multiferroic nanofibers, *Front. Phys.* 7(4), 399 (2012)
71. S. Ghasemi and A. Nematollahzadeh, Molecularly imprinted polymer membrane for the removal of naphthalene from petrochemical wastewater streams, *Adv. Polym. Technol.* 37(6), 2288 (2018)
72. K. Sanctucci and B. Shah, Association of naphthalene with acute hemolytic anemia, *Acad. Emerg. Med.* 7, 42 (2000)
73. A. Modak, M. Nandi, J. Mondal, and A. Bhaumik, Porphyrin based porous organic polymers: Novel synthetic strategy and exceptionally high CO_2 adsorption capacity, *Chem. Commun.* 48(2), 248 (2012)

74. X. He, Q. Shi, X. Zhou, C. Wan, and C. Jiang, In situ composite of nano SiO_2–P(VDF-HFP) porous polymer electrolytes for Li-ion batteries, *Electrochim. Acta* 51(6), 1069 (2005)
75. J. Y. Sanchez, F. Alloin, and C. P. Lepmi, Polymeric materials in energy storage and conversion, *Molecular Crystals and Liquid Crystals Science and Technology A* 324(1), 257 (1998)
76. M. Alamgir and K. M. Abraham, Li Ion Conductive Electrolytes Based on Poly(vinyl chloride), *J. Electrochem. Soc.* 140(6), L96 (1993)
77. Y. Wu, J. Wang, K. Jiang, and S. Fan, Applications of carbon nanotubes in high performance lithium ion batteries, *Front. Phys.* 9(3), 351 (2014)
78. Y. Huang, P. Liu, R. Hao, S. Kan, Y. Wu, H. Liu, and K. Liu, Engineering porous quasi-spherical Fe-N-C nanocatalysts with robust oxygen reduction performance for Zn-air battery application, *ChemNanoMat* 6(12), 1782 (2020)
79. J. Mandal, Y. Fu, A. C. Overvig, M. Jia, K. Sun, N. N. Shi, H. Zhou, X. Xiao, N. Yu, and Y. Yang, Hierarchically porous polymer coatings for highly efficient passive daytime radiative cooling, *Science* 362(6412), 315 (2018)
80. A. P. Raman, M. A. Anoma, L. Zhu, E. Rephaeli, and S. Fan, Passive radiative cooling below ambient air temperature under direct sunlight, *Nature* 515(7528), 540 (2014)
81. G. Sharma, B. Thakur, M. Naushad, A. Kumar, F. J. Stadler, S. M. Alfadul, and G. T. Mola, Applications of nanocomposite hydrogels for biomedical engineering and environmental protection, *Environ. Chem. Lett.* 16(1), 113 (2018)
82. W. Chen, S. Liu, Y. Dong, X. Zhou, and F. Zhou, Poly (m-phenylene isophthalamide)/graphene composite aerogels with enhanced compressive shape stability for thermal insulation, *J. Sol-Gel Sci. Technol.* 96(2), 370 (2020)
83. X. Han, J. Zhang, J. Huang, X. Wu, D. Yuan, Y. Liu, and Y. Cui, Chiral induction in covalent organic frameworks, *Nat. Commun.* 9, 1 (2018)
84. Z. Wang, G. Chen, and K. Ding, Self-supported catalysts, *Chem. Rev.* 109(2), 322 (2009)
85. C. Train, R. Gheorghe, V. Krstic, L. M. Chamoreau, N. S. Ovanesyan, G. L. J. A. Rikken, M. Gruselle, and M. Verdaguer, Strong magneto-chiral dichroism in enantiopure chiral ferromagnets, *Nat. Mater.* 7(9), 729 (2008)
86. S. G. Mosanenzadeh, S. Karamikamkar, Z. Saadatnia, C. B. Park, and H. E. Naguib, PPDA-PMDA polyimide aerogels with tailored nanostructure assembly for air filtering applications, *Separ. Purif. Tech.* 250, 117279 (2020)
87. S. Karamikamkar, H. E. Naguib, and C. B. Park, Advances in precursor system for silica-based aerogel production toward improved mechanical properties, customized morphology, and multifunctionality: A review, *Adv. Colloid Interface Sci.* 276, 102101 (2020)
88. Q. Qi, L. Ma, B. Zhao, S. Wang, X. Liu, Y. Lei, and C. B. Park, An effective design strategy for the sandwich structure of PVDF/GNP-Ni-CNT composites with remarkable electromagnetic interference shielding effectiveness, *ACS Appl. Mater. Interfaces* 12(32), 36568 (2020)
89. S. Liu, J. Gong, and B. Xu, Three-dimensionally conformal porous polymeric microstructures of fabrics for electrothermal textiles with enhanced thermal management, *Polymers (Basel)* 10(7), 748 (2018)
90. D. Reichenberg, Properties of ion-exchange resins in relation to their structure (III): Kinetics of exchange, *J. Am. Chem. Soc.* 75(3), 589 (1953)
91. B. Notario, J. Pinto, R. Verdejo, and M. A. Rodríguez-Pérez, Dielectric behavior of porous PMMA: From the micrometer to the nanometer scale, *Polymer (Guildf.)* 107, 302 (2016)
92. B. Zheng, X. Lin, X. Zhang, D. Wu, and K. Matyjaszewski, Emerging functional porous polymeric and carbonaceous materials for environmental treatment and energy storage, *Adv. Funct. Mater.* 30(41), 1907006 (2020)
93. H. Shin, S. Seo, C. Park, J. Na, M. Han, and E. Kim, Energy saving electrochromic windows from bistable low-HOMO level conjugated polymers, *Energy Environ. Sci.* 9(1), 117 (2016)
94. Y. Kim, M. Han, J. Kim, and E. Kim, Electrochromic capacitive windows based on all conjugated polymers for a dual function smart window, *Energy Environ. Sci.* 11(8), 2124 (2018)
95. S. Rashidi, J. A. Esfahani, and N. Karimi, Porous materials in building energy technologies — A review of the applications, modelling and experiments, *Renew. Sustain. Energy Rev.* 91, 229 (2018)
96. W. Chen and W. Liu, Thermal analysis on the cooling performance of a porous evaporative plate for building, *Heat Transf. Asian Res.* 39(2), 127 (2010)
97. N. Gupta and G. N. Tiwari, Review of passive heating/cooling systems of buildings, *Energy Sci. Eng.* 4(5), 305 (2016)
98. M. Dogru, M. Handloser, F. Auras, T. Kunz, D. Medina, A. Hartschuh, P. Knochel, and T. Bein, A photoconductive thienothiophene-based covalent organic framework showing charge transfer towards included fullerene, *Angew. Chem.* 125(10), 2992 (2013)
99. S. W. Park, Z. Liao, B. Ibarlucea, H. Qi, H. H. Lin, D. Becker, J. Melidonie, T. Zhang, H. Sahabudeen, L. Baraban, C. K. Baek, Z. Zheng, E. Zschech, A. Fery, T. Heine, U. Kaiser, G. Cuniberti, R. Dong, and X. Feng, Two-dimensional boronate ester covalent organic framework thin films with large single crystalline domains for a neuromorphic memory device, *Angew. Chem. Int. Ed.* 59(21), 8218 (2020)
100. Z. Lai, X. Guo, Z. Cheng, G. Ruan, and F. Du, Green synthesis of fluorescent carbon dots from cherry tomatoes for highly effective detection of trifluralin herbicide in soil samples, *Chemistry Select* 5(6), 1956 (2020)
101. M. D. Allendorf, R. Dong, X. Feng, S. Kaskel, D. Matoga, and V. Stavila, Electronic devices using open framework materials, *Chem. Rev.* 120(16), 8581 (2020)
102. F. Q. Huang, C. Y. Yang, and D. Y. Wan, Advanced solar materials for thin-film photovoltaic cells, *Front. Phys.* 6(2), 177 (2011)

103. S. B. Alahakoon, C. M. Thompson, G. Occhialini, and R. A. Smaldone, Design principles for covalent organic frameworks in energy storage applications, *ChemSusChem* 10(10), 2116 (2017)
104. G. A. Leith, A. M. Rice, B. J. Yarbrough, A. A. Berseneva, R. T. Ly, C. N. III Buck, D. Chusov, A. J. Brandt, D. A. Chen, B. W. Lamm, M. Stefik, K. S. Stephenson, M. D. Smith, A. K. Vannucci, P. J. Pellechia, S. Garashchuk, and N. B. Shustova, A dual threat: Redoxactivity and electronic structures of welldefined donoracceptor fulleretic covalentorganic materials, *Angew. Chem. Int. Ed.* 59(15), 6000 (2020)
105. J. Li, X. Jing, Q. Li, S. Li, X. Gao, X. Feng, and B. Wang, Bulk COFs and COF nanosheets for electrochemical energy storage and conversion, *Chem. Soc. Rev.* 49(11), 3565 (2020)
106. S. Lee, I. Y. Cho, D. Kim, N. K. Park, J. Park, Y. Kim, S. J. Kang, Y. Kim, and S. Y. Hong, Redox-active functional electrolyte for high-performance seawater batteries, *ChemSusChem* 13(9), 2220 (2020)
107. N. Liu, W. Li, M. Pasta, and Y. Cui, Nanomaterials for electrochemical energy storage, *Front. Phys.* 9(3), 323 (2014)
108. P. P. Mukherjee and C. Y. Wang, Direct numerical simulation modeling of bilayer cathode catalyst layers in polymer electrolyte fuel cells, *J. Electrochem. Soc.* 154(11), B1121 (2007)
109. X. A. Zhang, S. Yu, B. Xu, M. Li, Z. Peng, Y. Wang, S. Deng, X. Wu, Z. Wu, M. Ouyang, and Y. H. Wang, Dynamic gating of infrared radiation in a textile, *Science* 363(6427), 619 (2019)
110. Q. Peng, J. E, J. Chen, W. Zuo, X. Zhao, and Z. Zhang, Investigation on the effects of wall thickness and porous media on the thermal performance of a non-premixed hydrogen fueled cylindrical micro combustor, *Energy Convers. Manage.* 155, 276 (2018)
111. Y. Cui, H. Gong, Y. Wang, D. Li, and H. Bai, A thermally insulating textile inspired by polar bear hair, *Adv. Mater.* 30(14), 1706807 (2018)
112. Y. N. Song, Y. Li, D. X. Yan, J. Lei, and Z. M. Li, Novel passive cooling composite textile for both outdoor and indoor personal thermal management, *Compos. Part A Appl. Sci. Manuf.* 130, 105738 (2020)
113. R. Hu, Y. Liu, S. Shin, S. Huang, X. Ren, W. Shu, J. Cheng, G. Tao, W. Xu, R. Chen, and X. Luo, Emerging materials and strategies for personal thermal management, *Adv. Energy Mater.* 10(17), 1903921 (2020)
114. Y. Guo, C. Dun, J. Xu, J. Mu, P. Li, L. Gu, C. Hou, C. A. Hewitt, Q. Zhang, Y. Li, D. L. Carroll, and H. Wang, Ultrathin, washable, and large-area graphene papers for personal thermal management, *Small* 13(44), 1702645 (2017)
115. G. Dai, Designing nonlinear thermal devices and metamaterials under the Fourier law: A route to nonlinear thermotics, *Front. Phys.* 16, 1 (2021)
116. L. Qiu, N. Zhu, Y. Feng, E. E. Michaelides, G. Żyła, D. Jing, X. Zhang, P. M. Norris, C. N. Markides, and O. Mahian, A review of recent advances in thermophysical properties at the nanoscale: From solid state to colloids, *Phys. Rep.* 843, 1 (2020)
117. G. Xu, K. Dong, Y. Li, H. Li, K. Liu, L. Li, J. Wu, and C. Qiu, Tunable analog thermal material, *Nat. Commun.* 11, 1 (2020)
118. M. Chen, D. Pang, J. Mandal, X. Chen, H. Yan, Y. He, N. Yu, and Y. Yang, Designing mesoporous photonic structures for high-performance passive daytime radiative cooling, *Nano Lett.* 21(3), 1412 (2021)
119. T. Wang, M. C. Long, H. B. Zhao, B. W. Liu, H. G. Shi, W. L. An, S. L. Li, S. M. Xu, and Y. Z. Wang, An ultralow-temperature superelastic polymer aerogel with high strength as a great thermal insulator under extreme conditions, *J. Mater. Chem. A Mater. Energy Sustain.* 8(36), 18698 (2020)
120. F. Hu, S. Wu, and Y. Sun, Hollow-structured materials for thermal insulation, *Adv. Mater.* 31(38), 1801001 (2019)
121. Y. Guo, Z. Zhang, M. Bescond, S. Xiong, M. Nomura, and S. Volz, Anharmonic phonon-phonon scattering at the interface between two solids by nonequilibrium Green's function formalism, *Phys. Rev. B* 103(17), 174306 (2021)
122. G. Wang, C. Wang, J. Zhao, G. Wang, C. B. Park, and G. Zhao, Modelling of thermal transport through a nanocellular polymer foam: toward the generation of a new superinsulating material, *Nanoscale* 9(18), 5996 (2017)
123. G. Wang, C. Wang, J. Zhao, G. Wang, C. B. Park, G. Zhao, W. Van De Walle, and H. Janssen, Correction: Modelling of thermal transport through a nanocellular polymer foam: Toward the generation of a new superinsulating material, *Nanoscale* 10(43), 20469 (2018)
124. E. Cuce, C. H. Young, and S. B. Riffat, Performance investigation of heat insulation solar glass for low-carbon buildings, *Energy Convers. Manage.* 88, 834 (2014)
125. Y. Xu, L. Lin, M. Xiao, S. Wang, A. T. Smith, L. Sun, and Y. Meng, Synthesis and properties of CO_2-based plastics: Environmentally-friendly, energy-saving and biomedical polymeric materials, *Prog. Polym. Sci.* 80, 163 (2018)
126. J. Weng, D. Ouyang, X. Yang, M. Chen, G. Zhang, and J. Wang, Alleviation of thermal runaway propagation in thermal management modules using aerogel felt coupled with flame-retarded phase change material, *Energy Convers. Manage.* 200, 112071 (2019)
127. I. Oropeza-Perez and P. A. Østergaard, Active and passive cooling methods for dwellings: A review, *Renew. Sustain. Energy Rev.* 82, 531 (2018)
128. S. Kashyap, S. Kabra, and B. Kandasubramanian, Graphene aerogel-based phase changing composites for thermal energy storage systems, *J. Mater. Sci.* 55(10), 4127 (2020)
129. https://spinoff.nasa.gov/spinoff2001/ch5.html
130. P. R. Ferrer, A. Mace, S. N. Thomas, and J. W. Jeon, Nanostructured porous graphene and its composites for energy storage applications, *Nano Converg.* 4, 1 (2017)
131. E. Pakdel, M. Naebe, L. Sun, and X. Wang, Advanced functional fibrous materials for enhanced thermoregulating performance, *ACS Appl. Mater. Interfaces* 11(14), 13039 (2019)

132. A. Yang, L. Cai, R. Zhang, J. Wang, P. C. Hsu, H. Wang, G. Zhou, J. Xu, and Y. Cui, Thermal management in nanofiber-based face mask, *Nano Lett.* 17(6), 3506 (2017)
133. Y. Yang and Y. Zhang, Passive daytime radiative cooling: Principle, application, and economic analysis, *MRS Energy Sustain.* 7, 18 (2020)
134. M. Alvarez-Lainez, M. A. Rodriguez-Perez, and J. A. DE Saja, Thermal conductivity of open-cell polyolefin foams, *J. Polym. Sci. B Polym. Phys.* 46(2), 212 (2008)
135. L. R. Glicksman, in: Low Density Cellular Plastics, Springer Netherlands, 1994, pp 104–152
136. P. Buahom, C. Wang, M. Alshrah, G. Wang, P. Gong, M. P. Tran, and C. B. Park, Wrong expectation of superinsulation behavior from largely-expanded nanocellular foams, *Nanoscale* 12(24), 13064 (2020)
137. L. R. Glicksman, M. Torpey, and A. Marge, Means to improve the thermal conductivity of foam insulation, *J. Cell. Plast.* 28(6), 571 (1992)
138. A. G. Leach, The thermal conductivity of foams (I): Models for heat conduction, *J. Phys. D Appl. Phys.* 26(5), 733 (1993)
139. M. A. Schuetz and L. R. Glicksman, A basic study of heat transfer through foam insulation, *J. Cell. Plast.* 20(2), 114 (1984)
140. Z. M. Zhang, Nano/Microscale Heat Transfer, New York: McGraw-Hill, 2007
141. Y. L. He and T. Xie, Advances of thermal conductivity models of nanoscale silica aerogel insulation material, *Appl. Therm. Eng.* 81, 28 (2015)
142. T. Xie, Y. L. He, and Z. J. Hu, Theoretical study on thermal conductivities of silica aerogel composite insulating material, *Int. J. Heat Mass Transf.* 58(1–2), 540 (2013)
143. B. Notario, J. Pinto, E. Solorzano, J. A. De Saja, M. Dumon, and M. A. Rodríguez-Pérez, Experimental validation of the Knudsen effect in nanocellular polymeric foams, *Polymer (Guildf.)* 56, 57 (2015)
144. V. Bernardo, J. Martin-de Leon, J. Pinto, R. Verdejo, and M. A. Rodriguez-Perez, Modeling the heat transfer by conduction of nanocellular polymers with bimodal cellular structures, *Polymer (Guildf.)* 160, 126 (2019)
145. L. Wu, A slip model for rarefied gas flows at arbitrary Knudsen number, *Appl. Phys. Lett.* 93(25), 253103 (2008)
146. T. Inamuro, M. Yoshino, and F. Ogino, Accuracy of the lattice Boltzmann method for small Knudsen number with finite Reynolds number, *Phys. Fluids* 9(11), 3535 (1997)
147. S. Fukui and R. Kaneko, A database for interpolation of Poiseuille flow rates for high Knudsen number Lubrication problems, *J. Tribol.* 112(1), 78 (1990)
148. F. Tao and L. Nguyen, Interactions of gaseous molecules with X-ray photons and photoelectrons in AP-XPS study of solid surface in gas phase, *Phys. Chem. Chem. Phys.* 20(15), 9812 (2018)
149. D. R. Snelling, F. Liu, G. J. Smallwood, and Ö. L. Gülder, Determination of the soot absorption function and thermal accommodation coefficient using low-fluence LII in a laminar coflow ethylene diffusion flame, *Combust. Flame* 136(1–2), 180 (2004)
150. K. J. Daun, Thermal accommodation coefficients between polyatomic gas molecules and soot in laser-induced incandescence experiments, *Int. J. Heat Mass Transf.* 52(21–22), 5081 (2009)
151. G. Torzo, G. Delfitto, B. Pecori, and P. Scatturin, A new microcomputer-based laboratory version of the Rüchardt experiment for measuring the ratio $\gamma = C_p/C_v$ in air, *Am. J. Phys.* 69(11), 1205 (2001)
152. M. Pyda and B. Wunderlich, Computation of heat capacities of liquid polymers, *Macromolecules* 32(6), 2044 (1999)
153. G. Reichenauer, U. Heinemann, and H. P. Ebert, Relationship between pore size and the gas pressure dependence of the gaseous thermal conductivity, *Colloids Surf. A Physicochem. Eng. Asp.* 300(1–2), 204 (2007)
154. S. Q. Zeng, A. Hunt, and R. Greif, Mean free path and apparent thermal conductivity of a gas in a porous medium, *J. Heat Transfer* 117(3), 758 (1995)
155. G. Lu, X. D. Wang, Y. Y. Duan, and X. W. Li, Effects of non-ideal structures and high temperatures on the insulation properties of aerogel-based composite materials, *J. Non-Cryst. Solids* 357(22–23), 3822 (2011)
156. S. Q. Zeng, A. J. Hunt, W. Cao, and R. Greif, Pore size distribution and apparent gas thermal conductivity of silica aerogel, *J. Heat Transfer* 116(3), 756 (1994)
157. C. Bi, G. H. Tang, and W. Q. Tao, Prediction of the gaseous thermal conductivity in aerogels with non-uniform pore-size distribution, *J. Non-Cryst. Solids* 358(23), 3124 (2012)
158. J. Fricke, X. Lu, P. Wang, D. Büttner, and U. Heinemann, Optimization of monolithic silica aerogel insulants, *Int. J. Heat Mass Transf.* 35(9), 2305 (1992)
159. J. Lee, J. Lim, and P. Yang, Ballistic phonon transport in holey silicon, *Nano Lett.* 15(5), 3273 (2015)
160. G. Chen, Nonlocal and nonequilibrium heat conduction in the vicinity of nanoparticles, *J. Heat Transfer* 118(3), 539 (1996)
161. M. Alshrah, L. H. Mark, C. Zhao, H. E. Naguib, and C. B. Park, Nanostructure to thermal property relationship of resorcinol formaldehyde aerogels using the fractal technique, *Nanoscale* 10(22), 10564 (2018)
162. O. J. Lee, K. H. Lee, T. Jin Yim, S. Young Kim, and K. P. Yoo, Determination of mesopore size of aerogels from thermal conductivity measurements, *J. Non-Cryst. Solids* 298(2–3), 287 (2002)
163. Z. Deng, J. Wang, A. Wu, J. Shen, and B. Zhou, High strength SiO_2 aerogel insulation, *J. Non-Cryst. Solids* 225, 101 (1998)
164. S. Spagnol, B. Lartigue, A. Trombe, and V. Gibiat, Thermal modeling of two-dimensional periodic fractal patterns, an application to nanoporous media, *Europhysics Letters (EPL)* 78(4), 46005 (2007)
165. K. Swimm, G. Reichenauer, S. Vidi, and H. P. Ebert, Gas pressure dependence of the heat transport in porous solids with pores smaller than 10 μm, *Int. J. Thermophys.* 30(4), 1329 (2009)

166. S. Yang, J. Wang, G. Dai, F. Yang, and J. Huang, Controlling macroscopic heat transfer with thermal metamaterials: Theory, experiment and application, *Phys. Rep.* 908, 1 (2021)
167. J. Huang, Theoretical Thermotics: Transformation Thermotics and Extended Theories for Thermal Metamaterials, Springer, 2021
168. G. Wei, Y. Liu, X. Zhang, F. Yu, and X. Du, Thermal conductivities study on silica aerogel and its composite insulation materials, *Int. J. Heat Mass Transf.* 54(11–12), 2355 (2011)
169. J. J. Zhao, Y. Y. Duan, X. D. Wang, and B. X. Wang, An analytical model for combined radiative and conductive heat transfer in fiber-loaded silica aerogels, *J. Non-Cryst. Solids* 358(10), 1303 (2012)
170. W. L. Power and T. E. Tullis, Euclidean and fractal models for the description of rock surface roughness, *J. Geophys. Res.* 96(B1), 415 (1991)
171. R. Vacher, T. Woignier, J. Pelous, and E. Courtens, Structure and self-similarity of silica aerogels, *Phys. Rev. B* 37(11), 6500 (1988)
172. G. Edgar, Measure, Topology, and Fractal Geometry, Springer New York, 2008
173. B. B. Mandelbrot, The Fractal Geometry of Nature, New York: WH Freeman, 1982
174. G. Pia and U. Sanna, Intermingled fractal units model and electrical equivalence fractal approach for prediction of thermal conductivity of porous materials, *Appl. Therm. Eng.* 61(2), 186 (2013)
175. G. Pia and U. Sanna, An intermingled fractal units model to evaluate pore size distribution influence on thermal conductivity values in porous materials, *Appl. Therm. Eng.* 65(1–2), 330 (2014)
176. X. Huai, W. Wang, and Z. Li, Analysis of the effective thermal conductivity of fractal porous media, *Appl. Therm. Eng.* 27(17–18), 2815 (2007)
177. Y. Hayase and T. Ohta, Sierpinski gasket in a reaction-diffusion system, *Phys. Rev. Lett.* 81(8), 1726 (1998)
178. Y. Ma, B. Yu, D. Zhang, and M. Zou, A self-similarity model for effective thermal conductivity of porous media, *J. Phys. D Appl. Phys.* 36(17), 2157 (2003)
179. C. Jiang, K. Davey, and R. Prosser, A tessellated continuum approach to thermal analysis: Discontinuity networks., *Contin. Mech. Thermodyn.* 29(1), 145 (2017)
180. G. P. Saracco, G. Gonnella, D. Marenduzzo, and E. Orlandini, Equilibrium and dynamical behavior in the Vicsek model for self-propelled particles under shear, *Cent. Eur. J. Phys.* 10, 1109 (2012)
181. M. van den Berg, Heat equation on the arithmetic von Koch snowflake, *Probab. Theory Relat. Fields* 118(1), 17 (2000)
182. B. Yu and P. Cheng, Fractal models for the effective thermal conductivity of bidispersed porous media, *J. Thermophys. Heat Trans.* 16(1), 22 (2002)
183. T. Xie, Y. L. He, and Z. J. Hu, Theoretical study on thermal conductivities of silica aerogel composite insulating material, *Int. J. Heat Mass Transf.* 58(1–2), 540 (2013)
184. S. S. Sundarram and W. Li, On thermal conductivity of micro- and nanocellular polymer foams, *Polym. Eng. Sci.* 53(9), 1901 (2013)
185. Y. Amani, A. Takahashi, P. Chantrenne, S. Maruyama, S. Dancette, and E. Maire, Thermal conductivity of highly porous metal foams: Experimental and image based finite element analysis, *Int. J. Heat Mass Transf.* 122, 1 (2018)
186. Y. Amani and A. Öchsner, Finite element simulation of arrays of hollow sphere structures, *Materialwiss. Werkstofftech.* 46(4–5), 462 (2015)
187. H. Zhong and J. R. Lukes, Interfacial thermal resistance between carbon nanotubes: Molecular dynamics simulations and analytical thermal modeling, *Phys. Rev. B* 74(12), 125403 (2006)
188. S. G. Volz and G. Chen, Molecular dynamics simulation of thermal conductivity of silicon nanowires, *Appl. Phys. Lett.* 75(14), 2056 (1999)
189. W. Zhu, G. Zheng, S. Cao, and H. He, Thermal conductivity of amorphous SiO_2 thin film: A molecular dynamics study, *Sci. Rep.* 8, 1 (2018)
190. A. Henry and G. Chen, High thermal conductivity of single polyethylene chains using molecular dynamics simulations, *Phys. Rev. Lett.* 101(23), 235502 (2008)
191. Z. Y. Ong and E. Pop, Molecular dynamics simulation of thermal boundary conductance between carbon nanotubes and SiO_2, *Phys. Rev. B* 81(15), 155408 (2010)
192. P. K. Schelling, S. R. Phillpot, and P. Keblinski, Comparison of atomic-level simulation methods for computing thermal conductivity, *Phys. Rev. B* 65(14), 144306 (2002)
193. J. Che, T. Çagin, and W. A. III Goddard, Thermal conductivity of carbon nanotubes, *Nanotechnology* 11(2), 65 (2000)
194. A. J. H. McGaughey, and M. Kaviany, Thermal conductivity decomposition and analysis using molecular dynamics simulations, *Int. J. Heat Mass Transf.* 47(8–9), 1799 (2004)
195. Y. G. Yoon, R. Car, D. J. Srolovitz, and S. Scandolo, Thermal conductivity of crystalline quartz from classical simulations, *Phys. Rev. B* 70(1), 012302 (2004)
196. D. P. Sellan, E. S. Landry, J. E. Turney, A. J. H. McGaughey, and C. H. Amon, Size effects in molecular dynamics thermal conductivity predictions, *Phys. Rev. B* 81(21), 214305 (2010)
197. Y. F. Han, X. L. Xia, H. P. Tan, and H. D. Liu, Modeling of phonon heat transfer in spherical segment of silica aerogel grains, *Physica B* 420, 58 (2013)
198. T. Zeng and W. Liu, Phonon heat conduction in micro- and nano-core-shell structures with cylindrical and spherical geometries, *J. Appl. Phys.* 93(7), 4163 (2003)
199. A. Fakhari and T. Lee, Numerics of the lattice boltzmann method on nonuniform grids: Standard LBM and finite-difference LBM, *Comput. Fluids* 107, 205 (2015)
200. S. Chen and G. D. Doolen, Lattice Boltzmann method for fluid flows, *Annu. Rev. Fluid Mech.* 30(1), 329 (1998)
201. G. H. Tang, W. Q. Tao, and Y. L. He, Gas slippage effect on microscale porous flow using the lattice Boltzmann method, *Phys. Rev. E* 97, 104918 (2005)

202. Y. Peng, Y. T. Chew, and C. Shu, Numerical simulation of natural convection in a concentric annulus between a square outer cylinder and a circular inner cylinder using the Taylor-series-expansion and least-squares-based lattice Boltzmann method, *Phys. Rev. E* 67(2), 026701 (2003)
203. C. Y. Zhao, L. N. Dai, G. H. Tang, Z. G. Qu, and Z. Y. Li, Numerical study of natural convection in porous media (metals) using lattice Boltzmann method (LBM), *Int. J. Heat Fluid Flow* 31(5), 925 (2010)
204. H. Yu, H. Zhang, P. Buahom, J. Liu, X. Xia, and C. B. Park, Prediction of thermal conductivity of micro/nano porous dielectric materials: Theoretical model and impact factors, *Energy* 233, 121140 (2021)
205. S. Wang, Y. Huang, E. Chang, C. Zhao, A. Ameli, H. E. Naguib, and C. B. Park, Evaluation and modeling of electrical conductivity in conductive polymer nanocomposite foams with multiwalled carbon nanotube networks, *Chem. Eng. J.* 411, 128382 (2021)
206. A. Rizvi, R. K. M. Chu, and C. B. Park, Scalable fabrication of thermally insulating mechanically resilient hierarchically porous polymer foams, *ACS Appl. Mater. Interfaces* 10(44), 38410 (2018)
207. P. Gong, S. Zhai, R. Lee, C. Zhao, P. Buahom, G. Li, and C. B. Park, Environmentally Friendly Polylactic Acid-Based Thermal Insulation Foams Blown with Supercritical CO_2, *Ind. Eng. Chem. Res.* 57(15), 5464 (2018)
208. G. Wang, J. Zhao, G. Wang, L. H. Mark, C. B. Park, and G. Zhao, Low-density and structure-tunable microcellular PMMA foams with improved thermal-insulation and compressive mechanical properties, *Eur. Polym. J.* 95, 382 (2017)
209. J. R. Howell, R. Siegel, and M. P. Mengüç, Thermal Radiation Heat Transfer, 5th Ed., CRC Press, Taylor & Francis Group, 2010
210. Y. Feng and C. Wang, Discontinuous finite element method applied to transient pure and coupled radiative heat transfer, *Int. Commun. Heat Mass Transf.* 122, 105156 (2021)
211. T. Xie and Y. L. He, Heat transfer characteristics of silica aerogel composite materials: Structure reconstruction and numerical modeling, *Int. J. Heat Mass Transf.* 95, 621 (2016)
212. A. V. Gusarov, E. Poloni, V. Shklover, A. Sologubenko, J. Leuthold, S. White, and J. Lawson, Radiative transfer in porous carbon-fiber materials for thermal protection systems, *Int. J. Heat Mass Transf.* 144, 118582 (2019)
213. T. J. Hendricks and J. R. Howell, Absorption/scattering coefficients and scattering phase functions in reticulated porous ceramics, *J. Heat Transfer* 118(1), 79 (1996)
214. B. Quistián-Vázquez, B. Morales-Cruzado, E. Sarmiento-Gómez, and F. G. Pérez-Gutiérrez, Retrieval of absorption or scattering coefficient spectrum (RASCS) program: A tool to monitor optical properties in real time, *Lasers Surg. Med.* 52(6), 552 (2020)
215. F. Vaudelle, J. P. L'Huillier, and M. L. Askoura, Light source distribution and scattering phase function influence light transport in diffuse multi-layered media, *Opt. Commun.* 392, 268 (2017)
216. J. E. Sipe, New Green-function formalism for surface optics, *J. Opt. Soc. Am. B* 4(4), 481 (1987)
217. L. Dombrovsky, J. Randrianalisoa, and D. Baillis, Modified two-flux approximation for identification of radiative properties of absorbing and scattering media from directional-hemispherical measurements, *J. Opt. Soc. Am. A* 23(1), 91 (2006)
218. L. Dombrovsky, A. Leonid, G. Krithiga, and L. Wojciech, Combined two-flux approximation and Monte Carlo model for identification of radiative properties of highly scattering dispersed materials, *Comput. Therm. Sci.: Int. J.* 4, 4 (2012)
219. S. Chandrasekhar, The stability of non-dissipative Couette flow in hydromagnetics, *Proc. Natl. Acad. Sci. USA* 46(2), 253 (1960)
220. T. K. Kim, J. A. Menart, and H. S. Lee, Nongray radiative gas analyses using the S-N discrete ordinates method, *J. Heat Transfer* 113(4), 946 (1991)
221. R. Eymard, T. Gallouët, and R. Herbin, Finite volume methods, *Handbook Numer. Anal.* 7, 713 (2000)
222. A. Cohen, Wavelet methods in numerical analysis, *Handbook Numer. Anal.* 7, 417 (2000)
223. H. Yu, H. Zhang, Y. Guo, H. Tan, Y. Li, and G. Xie, Thermodynamic analysis of shark skin texture surfaces for microchannel flow, *Contin. Mech. Thermodyn.* 28(5), 1361 (2016)
224. H. Yu, H. Zhang, and X. Xia, A fractal-skeleton model of high porosity macroporous aluminum and its heat transfer characterizes, *J. Therm. Anal. Calorim.* 1, 1 (2020)
225. H. Yu, H. Zhang, C. Su, K. Wang, and L. Jin, The spectral radiative effect of Si/SiO_2 substrate on monolayer aluminum porous microstructure, *Therm. Sci.* 22(Suppl. 2), 629 (2018)
226. P. S. Cumber, Improvements to the discrete transfer method of calculating radiative heat transfer, *Int. J. Heat Mass Transf.* 38(12), 2251 (1995)
227. M. Fairweather, W. P. Jones, and R. P. Lindstedt, Predictions of radiative transfer from a turbulent reacting jet in a cross-wind, *Combust. Flame* 89(1), 45 (1992)
228. E. Solórzano, M. A. Rodriguez-Perez, J. Lázaro, and J. A. de Saja, Influence of solid phase conductivity and cellular structure on the heat transfer mechanisms of cellular materials: Diverse case studies, *Adv. Eng. Mater.* 11(10), 818 (2009)
229. L. R. Glicksman, T. Yule, and A. Dyrness, Prediction of the expansion of fluidized beds containing tubes, *Chem. Eng. Sci.* 46(7), 1561 (1991)
230. H. P. Tan, L. H. Liu, H. L. Yi, J. M. Zhao, H. Qi, and J. Y. Tan, Recent progress in computational thermal radiative transfer, *Chin. Sci. Bull.* 54(22), 4135 (2009)
231. S. Basu and Z. M. Zhang, Maximum energy transfer in near-field thermal radiation at nanometer distances, *J. Appl. Phys.* 105(9), 093535 (2009)
232. V. Bernardo, J. Martin-de Leon, J. Pinto, U. Schade, and M. A. Rodriguez-Perez, On the interaction of infrared radiation and nanocellular polymers: First experimental determination of the extinction coefficient, *Colloids Surf. A* 600, 124937 (2020)

233. J. Martín-de León, J. L. Pura, V. Bernardo, and M. Á. Rodríguez-Pérez, Transparent nanocellular PMMA: Characterization and modeling of the optical properties, *Polymer (Guildf.)* 170, 16 (2019)

234. C. F. Bohren and D. R. Huffman, Absorption and Scattering of Light by Small Particles, Wiley, Hoboken, 2004

235. M. Nieto-Vesperinas, Fundamentals of Mie scattering, Woodhead Publishing, 2020

236. S. Shen, A. Narayanaswamy, and G. Chen, Surface phonon polaritons mediated energy transfer between nanoscale gaps, *Nano Lett.* 9(8), 2909 (2009)

237. S. Shen, A. Henry, J. Tong, R. Zheng, and G. Chen, Polyethylene nanofibres with very high thermal conductivities, *Nat. Nanotechnol.* 5(4), 251 (2010)

238. X. Liu, L. Wang, and Z. M. Zhang, Near-field thermal radiation: Recent progress and outlook, *Nanoscale Microscale Thermophys. Eng.* 19(2), 98 (2015)

239. H. Yu, H. Zhang, H. Wang, and D. Zhang, The equivalent thermal conductivity of the micro/nano scaled periodic cubic frame silver and its thermal radiation mechanism analysis, *Energies* 14, 1 (2021)

240. B. Liu, F. Sun, X. Chen, and X. Xia, Prediction of radiation spectra of composite with periodic micron porous structure, *Numer. Heat Transf. B* 78(1), 54 (2020)

241. S. M. Rytov, Y. A. Kravtsov, and V. I. Tatarski, Principles of Statistical Radiophysics, Springer-Verlag, 1987

242. H. Yu, H. Zhang, Z. Dai, and X. Xia, Design and analysis of low emissivity radiative cooling multilayer films based on effective medium theory, *ES Energy & Environment* 6, 69 (2019)

243. L. X. Ma, C. C. Wang, and J. Y. Tan, Light scattering by densely packed optically soft particle systems, with consideration of the particle agglomeration and dependent scattering, *Appl. Opt.* 58(27), 7336 (2019)

244. S. Basu, Z. Zhang, and C. Fu, Review of near-field thermal radiation and its application to energy conversion, *Int. J. Energy Res.* 33(13), 1203 (2009)

245. X. Wu, C. Fu, and Z. M. Zhang, Effect of orientation on the directional and hemispherical emissivity of hyperbolic metamaterials, *Int. J. Heat Mass Transf.* 135, 1207 (2019)

246. M. Born and E. Wolf, Principles of Optics: Electromagnetic Theory of Propagation, Interference and Diffraction of Light, Elsevier, 2013